

MEMBRANE FILTRATION OF CRUDE OIL EMULSIONS STABILIZED BY COREXIT  
9500 DISPERSANT

By

SEYMA KUCUK

A THESIS

Submitted to  
Michigan State University  
in partial fulfillment of the requirements  
for the degree of

Environmental Engineering – Master of Science

2018

## ABSTRACT

### MEMBRANE FILTRATION OF CRUDE OIL EMULSIONS STABILIZED BY COREXIT 9500 DISPERSANT

By

SEYMA KUCUK

During the 2010 Deepwater Horizon oil spill, nearly 800 million liters of oil were released into the Gulf of Mexico polluting the deep ocean and more than 1600 km of the Gulf's shoreline. A large amount (7 million liters) of oil dispersant, Corexit EC 9500A, was applied to the spill; as a result, the oil was emulsified into microdroplets that remained suspended in the water column. Even though small droplets biodegrade faster, they can pose significant environmental risks. Microfiltration is the one of the most cost-effective remediation technologies that can remove emulsified oil. The present work is the first study of membrane filtration of Corexit-stabilized crude oil emulsions where properties and filterability of the emulsions in aqueous solutions of different salinities are evaluated. Salinity of the continuous phase was altered by adding  $\text{MgSO}_4$ ,  $\text{NaCl}$ , or a synthetic sea salt mixture. Emulsions were characterized in terms of their droplet size distribution, interfacial tension, and zeta potential. Corexit altered both emulsion stability and the wetting properties of the membranes. Emulsion characterization and constant pressure stirred dead-end filtration tests revealed that salinity affects the stability of emulsions and can enhance microfiltration performance. Almost complete rejection of oil was achieved but was accompanied by a precipitous flux decline. The low values of the steady state permeate flux indicate that microfiltration is suitable as a polishing step that follows an extensive pretreatment by large throughput deoiling unit processes such as hydrocyclonic separation or flotation.

Copyright by  
SEYMA KUCUK  
2018

## ACKNOWLEDGMENTS

To my family, thank you for your support.

To my advisor, Dr. Volodymyr Tarabara, thank you for your guidance and support.

To my committee members, Dr. Andre Benard and Dr. Phanikumar Mantha , thank you for your guidance.

To the former and current members of our research group especially Charifa Hejase, thank you for your help and positive attitude.

To Dr. Iryna S. Kolesnyk, thank you for your help and valuable contribution to this study.

To Turkish Petroleum Corporation, thank you for your supporting my MS study.

## TABLE OF CONTENTS

LIST OF TABLES .....	vii
LIST OF FIGURES .....	viii
KEY TO SYMBOLS AND ABBREVIATIONS .....	x
CHAPTER ONE .....	1
REFERENCES.....	7
CHAPTER TWO.....	10
2.1. Introduction .....	10
2.2. Materials and Methods.....	14
2.2.1 Reagents.....	14
2.2.2 Preparation and characterization of oil-water emulsions .....	14
2.2.3 Characterization of oil-water emulsions.....	16
2.2.4 Membranes used in dead-end microfiltration and DOTM tests.....	17
2.2.5 Membranes characterization .....	17
2.2.6 Dead-end microfiltration system .....	18
2.2.7 Direct observation through the membrane (DOTM) system .....	19
2.2.8 Measurement of crude oil concentration .....	20
2.3. Results and Discussion.....	21
2.3.1 Characteristics of oil-in-water emulsions .....	21
2.3.2 Membrane selection and characterization .....	27
2.3.3 Assessing filterability of crude oil emulsions.....	31
2.3.4 DOTM Tests .....	37
2.4. Conclusions .....	43
APPENDICES .....	45
APPENDIX A .....	46
APPENDIX B .....	47
APPENDIX C .....	48
REFERENCES.....	49

CHAPTER THREE .....	56
3.1. Introduction .....	56
3.2. Materials and Methods.....	60
3.2.1. Reagents .....	60
3.2.2 Preparation and characterization of oil-water emulsions .....	60
3.2.3 Measurement of hexadecane concentration .....	61
3.2.4 Dead-end microfiltration system .....	62
3.2.5. Membrane characterization .....	62
3.3. Results and Discussion.....	63
3.3.1 Characteristics of oil-in-water emulsions .....	63
3.3.2 Assessing filterability of hexadecane.....	69
3.4. Conclusions .....	73
APPENDIX D .....	74
REFERENCES.....	75

## LIST OF TABLES

Table 1: Direct observation through the membrane (DOTM) tests carried out with two different PCTE membranes and two Corexit-stabilized crude oil emulsions. ....	20
Table 2: Contact angles of air and crude oil with the PVP-coated PCTE membrane in different solutions. ....	28

## LIST OF FIGURES

Figure 1.1: The effects of Corexit 9500A on the interfacial tension of crude oil emulsions in deionized water and in synthetic sea water. ....	23
Figure 1.2: Volume-based (a) and number-based (b) droplet size distributions of Corexit-stabilized crude oil emulsions, 1000-10-0 and 1000-10-IO, in synthetic sea water and deionized water. The concentration of the oil and the CE9500 dispersant are 1000 $\mu\text{L}(\text{oil})/\text{L}$ and 10 $\mu\text{L}(\text{CE9500})/\text{L}$ . The same emulsions were used in constant pressure microfiltration tests. ....	26
Figure 1.3: Critical transmembrane pressure required as a function of oil droplet size. Critical pressure is the pressure required for a droplet to enter a membrane pore. The calculation is based on eq. (1) and is for crude oil and a membrane with the nominal pore size of 0.40 $\mu\text{m}$ , interfacial tension, $\sigma$ , of $21.84 \pm 0.2 \text{ mN/m}$ (in sea water) and the contact angle $\phi$ , of $149.4^\circ \pm 0.1^\circ$ (in sea water). ....	30
Figure 1.4: Permeate flux behavior in dead-end microfiltration tests with Corexit-stabilized crude oil emulsions. The experiments were performed in a constant pressure regime ( $\Delta P = 2 \text{ psi}$ ). The hydraulic resistance of clean membranes averaged over the six tests was $(31 \pm 2) \cdot 10^9 \text{ m}^{-1}$ . ....	35
Figure 1.5: Transient behavior of Corexit 9500-stabilized crude oil droplets at the surface of 0.03 $\mu\text{m}$ pore size membrane in DI water (A – D) and in synthetic sea water (E – H). Images A and E correspond to $t = 0$ when the membrane is unfouled. The direction of crossflow (0.1. m/s) is from left to right in all DOTM images ....	39
Figure 1.6: Behavior of Corexit 9500-stabilized crude oil droplets at the surfaces of 0.03 $\mu\text{m}$ and 0.2 $\mu\text{m}$ pore size membranes in DI water and in synthetic sea water ....	40
Figure 1.7: Transient behavior of Corexit 9500-stabilized crude oil droplets at the surface of 0.2 $\mu\text{m}$ pore size membrane in DI water (A – D) and in synthetic sea water (E – H). Images A and E correspond to $t = 0$ when the membrane is unfouled. The direction of crossflow (0.1. m/s) is from left to right in all DOTM images. ....	42
Figure 2.1: Volume and Number fraction (%) distributions for SDS-stabilized hexadecane-water emulsion 1000 $\mu\text{L}(\text{oil})/\text{L}$ , 0.1mM SDS in different salinities.....	65
Figure 2.2: Volume and Number fraction (%) distributions for SDS-stabilized hexadecane-water emulsion 1000 $\mu\text{L}(\text{oil})/\text{L}$ , 0.1mM SDS in different salinity.....	66
Figure 2.3: Permeate flux behavior in dead-end microfiltration tests with SDS-stabilized hexadecane emulsions in either DI or model sea water. The experiments were performed in a constant pressure regime ( $\Delta P = 2 \text{ psi}$ ). The hydraulic resistance of	



membranes averaged over tests 1 – 3 with emulsions in DI and model water. Average hydraulic resistances of the membrane was  $(36 \pm 3) \cdot 10^9 \text{ m}^{-1}$  ..... 69

Figure 2.4: Permeate flux behavior in dead-end microfiltration tests with SDS-stabilized hexadecane emulsions in different  $\text{MgSO}_4$  concentrations. The experiments were performed in a constant pressure regime ( $\Delta P = 2 \text{ psi}$ ). The hydraulic resistance of membranes averaged over tests 1 – 3 with emulsions in 6.7 mM  $\text{MgSO}_4$  and 54.3 mM  $\text{MgSO}_4$ . Average hydraulic resistances of the membrane was  $(33 \pm 2) \cdot 10^9 \text{ m}^{-1}$  .....70

Figure A.1: Calibration curve for crude oil concentration determination.....46

Figure B.1: Permeate flux behavior in dead-end microfiltration tests with Corexit 9500-stabilized crude oil emulsions. Crude oil concentrations were 50  $\mu\text{L/L}$  and in the presence of model sea salt. Corexit concentration are 5 (50/5), 2.5 (50/2.5), 1 (50/1)  $\mu\text{L/L}$  and absence of Corexit 9500 (50/0). The experiments were performed in a constant pressure regime ( $\Delta P = 8 \text{ psi}$ ). The hydraulic resistance of clean membranes averaged was  $3.6 \times 10^{13} \text{ m}^{-1}$  .....47

Figure D.1: Calibration curve for hexadecane concentration determination ..... 74

## KEY TO SYMBOLS AND ABBREVIATIONS

°C	Degree Celsius
$\Delta P$	Transmembrane pressure (psi)
$d_{\text{drop}}$	Oil droplet diameter ( $\mu\text{m}$ )
$d_{\text{pore}}$	A circular pore diameter of membrane ( $\mu\text{m}$ )
$\phi$	Contact angle ( $^{\circ}$ )
M $\Omega$	Megohm
$\mu\text{L}$	Microliter
$\mu\text{m}$	Micrometer
mM	Millimolar
mN	Millinewton
mPa	Milipascal
mV	Millivolt
M	Molar
$\sigma$	Interfacial tension (mN/m)
$\Theta$	Contact angle ( $^{\circ}$ )
<sup>TM</sup>	Trademark
W	Watt
$\zeta$	Zeta potential (mV)
CMC	Critical micelle concentration (mg/L)
CE9500	Corexit EC9500A
DWH	Deepwater Horizon
DCM	Dichloromethane

DOTM	Direct observation through the membrane
DSD	Droplet size distribution
IFT	Interfacial tension (mN/m)
IO	Instant ocean salt
ppm	Parts per million
PTCE	Polycarbonate track-etch
PVP	Polyvinyl pyrrolidone
psi	Pounds per square inch
rpm	Revolutions per minute
TCB	Trichlorobenzene

## CHAPTER ONE

### A review of oily wastewater

The expansion in energy demands has led to an increase in water pollution. Huge quantity of oily wastewater was generated by oil-gas production, oil refining, oil storage, transportation and petrochemical industries. The largest byproduct associated with the exploration and production of oil and gas is produced water which is the primary source of oily wastewater [1]. Beside produced water, increase in offshore oil-gas production, exploration, and crude oil transportation have led to several major oil spill accidents such as; the 1989 Exxon Valdez, the 2010 Deepwater Horizon (DWH) oil spill and recently the East China Sea oil spill [2-4]. Raised in both produced water and oil spills have created a global awareness of the risks on environment. In parallel to this environmental concern, legislations about produced water have been getting more stringent. The United State Environmental Protection Agency (USEPA) set the daily maximum oil-grease discharged limit at 42 ppm and the annual average discharged limit into the sea was set at 40 ppm by the Protection of the Marine Environment of the North-East Atlantic [1, 5].

#### Produced Water

The amount of the produced water depends on natural water layer (formation water) in the reservoir and injected water into the reservoir to push oil to surface [6]. Its

characteristic might change with the influx of injection water and it varies depending on the type of hydrocarbon in the basin, geographic location and geological formation.

External fluids, which might be required to increase volumetric sweep efficiency and maintain pressure, can contain chemicals, miscible gases or the injection of thermal energy [1]. One of the major chemical is added to external fluids are surface-active agents (surfactant). The main purpose of surfactant usage is decreasing interfacial tension between oil and the fluid to enhance the oil recovery from the reservoir [6].

Surfactants are usually composed of a hydrocarbon chain (hydrophobic group, the “tail”) and a polar hydrophilic group (the “head”). While the tail refers to the lyophobic or hydrophobic group in water, the head refers to the lyophilic or hydrophilic group [7]. They are classified depending on the ionic nature of the head group which can be nonionic, anionic, cationic and zwitterionic. In enhanced oil recovery processes, anionic surfactants are commonly used due to relatively low adsorption on sandstone rocks which are negatively charged [8].

Produced water generally contains liquid or gaseous hydrocarbons, dissolved or suspended solids, sand or silt and production chemical such as surfactants and salinity which can vary 1,00 ppm to 250,000 ppm [9].

Injection, discharge, reuses in oil-gas operation or consume beneficial use are the several options for produced water management. Injection of the produced water into

formation comes with the concern of pollution of groundwater and it usually requires transportation of water and treatment to decrease fouling and bacterial growth. Besides, re-injection of the produced water, other options might be required treatment of the produced water. Chemical precipitation and oxidation, biological treatment, adsorption, sand filters, cyclones, evaporation, dissolved air precipitation, electrodialysis and membrane filtration are some of the methods to treat produced water. The common objectives to treat produced water are removing dispersed oil or organics, dissolved salts, light hydrocarbon gases, hardness, suspended particles, sand and naturally occurring radioactive materials. To meet required treatment based on regulation, operator generally applied combined treatment processes [1, 5].

## Oil Spills

Every year, large amount of oil spills to environment. ~ 3.7 million tons of oil spilled since 1970 and last year (2017) approximately 7,000 tons of oil spilled. Even if the amount of spilled oil decreases every decade, it is still high risk on environment [10].

Typical composition of crude oil includes alkanes, branched alkanes, cycloalkanes, olefins, monoaromatics and phenol. However, it is a complex mixture of thousands of organic compounds and its composition changes one source to another. Thus, the effects on the environment change with the changing source. Beside crude oil source, the effects of oil spills can vary depending on the environment where the spill occurred. The aquatic systems are one of the most sensitive environments and marine mammals, terrestrial mammals, birds, fish, invertebrates, reptiles and plants are highly vulnerable

to oil spill. They can be exposed a wide range of adverse effects which include reduced growth, impaired reproduction, impaired physiological health, behavioral changes, loss of habitat, and mortality [11].

Once oil spills into an aquatic system, its physical and chemical characteristics change. These processes are called weathering. Weathering processes and rate directly related to spill environment conditions and oil properties. For instance, high temperature and solar irradiance increase weathering rate. Regarding oil composition, light crude oil presents high evaporation, dissolution and biodegradation rate compare to heavy crude oils [12].

Weathering is a passive remediation way of oil. In order to control and treat oil spill, several mechanical, physical and chemical remediation techniques have been used. Mechanical recovery is the primary response to oil spill in the United States. Mostly, booms, barriers, skimmers and natural or synthetic sorbent materials are used for emergency response. Booms are used for controlling the oil spread and skimmers recover the oil from water surface. Physical methods such as pressure washing or wiping with sorbent materials are usually used for shoreline clean up. Dispersing agents and gelling agents are generally applied as chemical methods. The aim of chemical application is keeping away oil from shoreline and sensitive habitats [13].

Corexit EC9500A (CE9500) and Corexit EC9527 are the most common dispersants which are used in oil spills. During oil spills, these dispersants sprayed to sea surface by aircrafts. However, they were applied to undersea spill point in the Deepwater Horizon

oil spill in addition to surface application. The recommended dispersant to oil ratio is between 1:20 and 1:30 to achieve effective oil dispersion [14, 15].

#### Oily Wastewater Treatment by Membranes

Both produced water and oil spills cause large volume of oily wastewater. The characteristics of these waters such as, pH, salinity, properties of oil and oil droplet size have a key role on remediation of the oily wastewater and based on the wastewater character the treatment methods can vary.

Oil droplets are classified based on droplet size which is the one of the critical parameter to determine treatment method. While oil droplets bigger than 150  $\mu\text{m}$  which calls free oil, oil droplets with the size range of between 20  $\mu\text{m}$  and 150  $\mu\text{m}$  which are named dispersed oil. These types oil can be removed by gravity separator or gravity coalescing. However, once oil droplets smaller than 20  $\mu\text{m}$  which are called emulsified oil, removing of these oil droplets from water becomes more difficult and expensive [16]. Emulsified oil can be treated with the addition of chemical additives and further treatment. However, membrane filtration is very competitive with no chemical additive requirement and high removal efficiency [17].

Special porous materials with different pore sizes are used in membrane filtration. The treatment processes rely on the physical separation and pressure uses as driven force. Depending on pore size of membrane and applied pressure on membrane, separation processes divide into microfiltration, ultrafiltration, nanofiltration and reverse osmosis.



Membrane technology can overcome many challenges of oily wastewater treatment. It can supply high efficiency even the feed water character is varied with time. It does not require any chemical addition and it can apply for wide range of industrial oily wastewater. On the other hand, fouling is the major obstacle to widespread implementation of membrane filtration [18]. The studies about membrane fouling during the filtration of oily wastewater showed that the organic content of wastewater, such as oil and organic substance (TOC) might contribute the fouling [1, 19, 20]. Beside organic content of wastewater, it was revealed that membrane fouling is controlling by many parameters such as membrane pore size, hydrophilicity and roughness [21-23].

## REFERENCES

## REFERENCES

- [1] A. Fakhru'l-Razi, A. Pendashteh, A. Luqman Chuah, D. Radiah, S. Siavash Madaeni, Z. Abidin, Review of Technologies for Oil and Gas Produced Water Treatment, 2009.
- [2] G. Mullany, Huge oil spill spreads in East China Sea, stirring environmental fears, in, The New York Times, 2018.
- [3] D.M. Patten, Intra-industry environmental disclosures in response to the Alaskan oil spill: A note on legitimacy theory, 17 (1992) 471-475.
- [4] R. Weisberg, L. Zheng, Y. Liu, On the Movement of Deepwater Horizon Oil to Northern Gulf Beaches, 2017.
- [5] E.T. Igunnu, G.Z. Chen, Produced water treatment technologies, 9 (2014) 157-177.
- [6] D. Wandera, S.R. Wickramasinghe, S.M. Husson, Modification and characterization of ultrafiltration membranes for treatment of produced water, 373 (2011) 178-188.
- [7] D. Myers, Surfactant Science and Technology, 3rd ed., John Wiley & Sons, Inc., New Jersey, 2006.
- [8] J.J. Sheng, Chapter 7 - Surfactant Flooding, in, Gulf Professional Publishing, Boston, 2011, pp. 239-335.
- [9] R.L. Pitre, Produced Water Discharges into Marine Ecosystems, Offshore Technology Conference, (1984).
- [10] T.i.t.o.p.f. limited, Oil Tanker Spill Statistics, in, ITOPF, London, UK, 2017.
- [11] I. Onwurah, V. Ogugua, N. B. Onyike, A. Ochonogor, O.O. Olawale, Crude Oils Spills in the Environment, Effects and Some Innovative Clean-Up Biotechnologies, 2007.
- [12] Z. Liu, J. Liu, Q. Zhu, W. Wu, The weathering of oil after the Deepwater Horizon oil spill: Insights from the chemical composition of the oil from the sea surface, salt marshes and sediments, 2012.
- [13] EPA, EPA's Response Techniques, in.
- [14] EPA, Corexit EC9500A, in: Emergency Response.
- [15] D.L. Valentine, I. Mezić, S. Maćešić, N. Črnjarić-Žic, S. Ivić, P.J. Hogan, V.A. Fonoberov, S. Loire, Dynamic autoinoculation and the microbial ecology of a deep

water hydrocarbon irruption, Proceedings of the National Academy of Sciences, 109 (2012) 20286.

## CHAPTER TWO

### Membrane filtration of crude oil emulsions stabilized by Corexit 9500 dispersant

#### 2.1. Introduction

During the Deepwater Horizon (DWH) oil spill in 2010, approximately 800 million liters of oil were released from ~1.5 km water depth into the Gulf of Mexico and about half of the spilled oil remained in the deep sea [1, 2]. As a response action, 7 million liters of an oil dispersant was applied. While 4.1 million liters of oil dispersant were sprayed to the sea surface, 2.9 million liters were applied to undersea spill point to enhance production of smaller droplets with slower ascent rate [3, 4]. The dispersants were Corexit EC9500A and Corexit EC9527A, which are commonly used for oil spill remediation [5, 6]. The primary dispersant was Corexit EC9500A (hereinafter, CE9500), which is a mixture of nonionic surfactants (sorbitan monooleate (Span 80), sorbitan monooleate polyethoxylate (Tween 80), sorbitan trioleate polyethoxylate (Tween 85)) and anionic surfactant (dioctyl sodium sulfosuccinate(DOSS)) in a solvent which consists of 1-(2-butoxy-1-methylethoxy) propanol and light hydrocarbon distillates [7, 8]. It is newer formulation compare to Corexit 9527 and it works on wider range of oils. The only difference between two surfactants is solvent [9]. The exact chemical makeup of the dispersant is proprietary.

Dispersants adsorb at the oil-water interface and decrease the interfacial tension of the oil-water emulsion. Interfacial tension (the energy required for oil droplet break up)

decreased with a decrease in interfacial tension [10]. The effectiveness of surfactants can vary with the types of oil and surfactant, mixing conditions, temperature, and the composition of the dispersion medium (e.g. salinity, content of specific ions) [8, 11]. The charge of the dispersant-coated oil droplet depends on the charge of the hydrophilic head group of the dispersant [12]. However, nonionic surfactant can also be responsible for a charge by promoting adsorption of hydroxyl ions at the oil-water interface [13, 14]. In the case of CE9500-stabilized oil-water emulsions, the oil droplets carry a negatively charge [8, 15].

The presence of salt in the continuous phase leads to a decrease in the Debye length due to charge screening and results in reduction of droplet-droplet electrostatic repulsion [8, 16, 17] favoring droplet coalescence [17, 18]. The effect counteracts salt-induced decrease in the interfacial tension due to the salting out of the surfactant to the oil-water interface. In parallel to this effect, Shinoda et al. [19] explained the reduction of the interfacial tension in the presence of salt as resulting from a change in hydrophile-lipophile balance.

Because dispersants are mostly used to disperse oil in marine environments, the dispersant formulations are optimized for high salinities [20]. Blondina et al. observed a decrease in CE9500 effectiveness at the lower salinity of 15 ppt [20]. Powell et al. also reported decrease in the interfacial tension of CE9500 stabilized emulsion in the presence of sea water salt [21]. However, in some cases, salinity-induced mitigation of droplet-droplet electrostatic repulsion is more important than a decrease in the in

interfacial tension. For example, Tummons et al. did not observe a correlation between the interfacial tension and droplet size distribution in saline condition [22].

Under different conditions, droplet sizes of oil in water emulsions have been investigated [22-26]. Li et al. measured the droplet size of CE9500 stabilized crude oil emulsions [27]. They observed wide range oil droplet sizes including droplets are smaller than 10 $\mu$ m under regular and breaking wave conditions. Pan et al. revealed that in the presence of CE9500, the time and the mixing energy which are required for effective oil dispersion were less than the absence of CE9500 condition and they also measured smaller oil droplets in the presence of CE9500 [24].

Oil droplet size in an oil-water emulsion is a key parameter that determines the efficiency of oil-water separation. The efficiency of conventional processes such as flotation and hydrocyclonic separation decreases with a decrease in droplet size [28-30]. Droplets which are smaller than 10 $\mu$ m are not removed effectively by any of the conventional high-throughput separation method. De-emulsifiers increase droplet size and improve separation but chemical additives and further treatment [31] may not be acceptable options. Membrane filtration is an alternative technology that can ensure high oil removal efficiency [32, 33]. However, concentration polarization and membrane fouling remain two serious problems that limit boarder adoption of the membranes [32].

A number of prior studies focused on membrane fouling by emulsified oil [34, 35].

Factors that define dominant fouling mechanisms are pH, salinity, temperature, shear stress, pressure, feed concentration of the oil, oil droplet size and charge, surfactant type, membrane material and pore size [34, 36-38]. Zhu et al. revealed that oppositely charged surfactant and membrane surface resulted in quick membrane fouling due to electrostatic attraction. In the presence of salt, the interaction between oil droplets and membrane surface are affected. Zhu et al. [39] observed droplet penetration due to decrease of the surface tensions in the presence of salt. Tummons et al [22], observed the membrane surface during ultrafiltration of surfactant-stabilized emulsions in different aqueous, and reported enhanced droplet coalescence in the presence of salt.

In this paper, we aim to understand the effect of salinity on membrane fouling by emulsified crude oil. Permeate flux analysis as well as direct visualization were employed to understand the fouling behavior of CE9500-stabilized crude oil emulsions during microfiltration by an oleophobic membrane with 0.4  $\mu\text{m}$  pore size. Emulsions were characterized in terms of droplet size and charge, interfacial tension. Constant pressure dead-end filtration tests were conducted to understand the kinetics of permeate flux decline under different salinity conditions. Direct Observation Through the Membrane (DOTM) was used for real-time visualization of oil droplet behavior on the membrane surface.



## 2.2. Materials and Methods

### 2.2.1 Reagents

Tetracosane (99%) and 1,3,5-trichlorobenzene (99%) were purchased from Sigma-Aldrich. Dichloromethane and potassium chloride (KCl, 99%) were purchased from J.T. Baker. Synthetic sea salt mixture (Instant Ocean<sup>TM</sup>) was purchased from Petco. Hydrochloric acid (HCl, EMD Chemicals) was diluted to 1 M. Deionized (DI) water was produced by a Milli-Q ultrapure water system (Integral 10, Millipore) equipped with a terminal 0.2  $\mu\text{m}$  microfilter (MilliPak, Millipore); the water resistivity was  $\sim 18 \text{ M}\Omega\cdot\text{cm}$  [39].

Crude oil and Corexit EC9500A (Nalco Environmental Solutions, LLC) were provided by the National Oceanic and Atmospheric Administration. Crude oil samples were collected by Helix Producer (a Floating Production vessel) on August 18, 2010 from the wellhead at the site of the Deepwater Horizon spill in support of the spill response and the Natural Resource Damage Assessment. The samples were made available to the broader research community in 2016 after the legal case was settled and the assessment was complete.

### 2.2.2 Preparation and characterization of oil-water emulsions

The emulsions were prepared by adding crude oil to the solution of CE9500 in either DI water or in synthetic sea water. The crude oil dynamic viscosity was measured to be

3.09 mPa·s at 20°C by Cannon-Fenske routine viscometer (Cannon Instrument Co.).

The content of crude oil in all emulsions was 0.1% v/v (1000 µL/L). The concentration of CE9500 was 0.001% v/v (10 µL/L) so that the oil-to-dispersant volume ratio was 100:1.

The synthetic sea water was prepared by adding 35.789 g of the Instant Ocean salt to 1 L of the DI water.

The solutions used for membrane conditioning were oil-free and contained either the same concentration of salt or the same concentration of CE9500 as the emulsions.

Emulsions were prepared by mixing 1 L of the oil-water-surfactant mixture at 1,000 rpm using a digital stand mixer (RW 20 digital dual range-mixer, IKA) for 20 min. The mixing conditions correspond to the energy dissipation rate of 1.82 W/kg, which is within the 1 to 10 W/kg range reported for breaking wave conditions [40].

For the DOTM tests, the non-saline emulsion was prepared by adding crude oil to the water in the presence of CE9500 dispersant as a stabilizing agent. The crude oil concentration was 0.01% v/v (74.5 mg/L) while Corexit concentration was similar to the emulsions used in the dead-end filtration tests. In addition, the mixing conditions were the same as those used to prepare emulsions used in dead-end microfiltration tests.

The only difference between the saline and non-saline emulsions was the addition of 35.789 g of Instant Ocean sea salt mixture. In what follows, the emulsions are referred to as X-Y-Z, where X and Y are the contents of oil and Corexit in µL per L of water, respectively, and Z is “0” or “IO” depending on whether the oil is dispersed in DI water or in the Instant Ocean solution.

### 2.2.3 Characterization of oil-water emulsions

Light diffraction (Malvern Mastersizer 2000) was used to measure droplet size distribution of emulsions. The refractive index for crude oil was 1.453 [41]. During droplet size measurements, the emulsions were circulated from the sample dispersion unit stirred at 1,000 rpm, through the optical cell of the particle sizer and back into the dispersion unit. The volume-based distributions were directly reported by instrument's software and the number-based distributions were calculated based on the volume-based data. Surface tension and interfacial tension were measured by a standard goniometer (model 250-F4, rame-hart instrument co.) at the room temperature. The pendant drop technique was used for the surface tension measurements of either pure liquids (crude oil, water) or solutions. The data was used as inputs to the DROPImage Advanced software for the measurements of interfacial tension of emulsions. The microsyringe was used to produce a pendant droplet, and surface tension was determined based on the shape of the droplet by the software. For interfacial tension measurements, the microsyringe with inverted stainless steel 22g needle was filled with crude oil and used to produce a pendant droplet inside the quartz cell (part 100-07-50, rame-hart instrument co.) with aqueous solutions of CE9500. The interfacial tension was quantified by the software based on the droplet's shape. Phase analysis light scattering (Zeta PALS, Brookhaven Instruments) was employed to measure zeta potential of oil droplets in presence of CE9500. The background electrolyte was 1 mM KCl.

#### 2.2.4 Membranes used in dead-end microfiltration and DOTM tests

Polyvinyl pyrrolidone (PVP) coated polycarbonate track-etch (PCTE) membranes with a nominal pore size of 0.40  $\mu\text{m}$  were used in all dead-end microfiltration tests. Two other types of hydrophilic PCTE membranes (Sterlitech) were used during the DOTM tests: an ultrafilter and a microfilter with nominal pore sizes of 0.03  $\mu\text{m}$  and 0.2  $\mu\text{m}$ , respectively; both of these PCTE membranes are optically transparent when wet, which is a requirement of the DOTM method. A new membrane was used in each dead-end filtration and each DOTM test. The track-etch membranes have cylindrical straight-through pores with very narrow pore size distribution making them a suitable choice for mechanistic studies of membrane fouling. The surface porosity of these membranes, however, is low - 0.42% and 9.43%, respectively (see SM: section SM1 and Table S1), leading to permeate fluxes that are lower than that of commercially used membranes of the same nominal pore size.

#### 2.2.5 Membranes characterization

Contact angles of crude oil on the membrane surface were determined by the goniometer for each solution. A solution of CE9500 in either synthetic sea water or DI water was added to the standard quartz cell. The membrane was attached to the environmental fixture (part 100-14, rame-hart instrument co.) with the feed side facing downward and submerged in the solution. The oil droplet was released below the membrane by the inverted stainless steel 22g needle until the droplet attached to the

membrane. The contact angle of the oil droplet on the submerged membrane surface in various solutions was determined by DROPImage Advanced software based on the shape of the droplet.

The same captive bubble method was used to determine the contact angle of air bubble on the membrane surface. The air bubble released below the membrane by the syringe attached the membrane's feed surface. The attached air bubble's contact angle was measured by DROPImage Advanced software based on the shape of the bubble.

#### 2.2.6 Dead-end microfiltration system

A hydrophilic polycarbonate track-etch (PTCE) membrane with a nominal size of 0.40  $\mu\text{m}$  was used in all microfiltration tests. Microfiltration of crude oil emulsions was conducted at the constant transmembrane pressure,  $\Delta P$ , of 2 psi using a stainless-steel filtration cell (HP 4750, Sterlitech Corp.) stirred with magnetic stirrer at  $\sim 510$  rpm. Electronic mass balance (Adventurer Pro AV812, OHAUS Corp.) was used to continuously record permeate mass. Prior to each filtration experiment, a clean water flux test ( $\Delta P = 1, 2, 3$  and 4 psi) and conditioning with aqueous solutions of CE9500 were performed.

### 2.2.7 Direct observation through the membrane (DOTM) system

A detailed description of the DOTM setup has been provided earlier [42, 43]. Briefly, the main feature of the DOTM system is the microscope (Axio Imager. M1, Zeiss) that is equipped with a video camera (Digital Color video camera model TK-C921BEG, JVC) capable of capturing still images and videos. The active membrane area was  $2.4 \text{ cm}^2$  and was located in the middle of the crossflow channel with the permeate side facing the microscope's objective. Images were captured by focusing the light emitted by the microscope's illuminator through the membrane and onto its feed side.

The  $0.4 \text{ }\mu\text{m}$  PCTE membranes used in crossflow filtration experiments were not sufficiently transparent to be used in DOTM tests. Thus, PCTE membranes with pore sizes of  $0.03 \text{ }\mu\text{m}$  and  $0.2 \text{ }\mu\text{m}$  were selected (Table 1); both membranes were optically transparent when wetted by water.

The 1000-10-0 and 1000-10-IO emulsions used in crossflow filtration experiments could not be used in DOTM tests. Throughout each DOTM experiment, the feed emulsion in the feed tank was mixed by a magnetic stir bar and the retentate was cycled back to the tank. The permeate flux was maintained constant using a peristaltic permeate pump (Minipuls 3, Gilson). All DOTM tests were done at a constant crossflow velocity of  $3.6 \cdot 10^5 \text{ L} \cdot \text{m}^{-2} \cdot \text{h}$  ( $0.1 \text{ m/s}$ ).

Table 1: Direct observation through the membrane (DOTM) tests carried out with two different PCTE membranes and two Corexit-stabilized crude oil emulsions.

Emulsion Membrane	100-10-0	100-10-IO
0.03 $\mu\text{m}$ PCTE	DOTM Test 1	DOTM Test 2
0.2 $\mu\text{m}$ PCTE	DOTM Test 3	DOTM Test 4

## 2.2.8 Measurement of crude oil concentration

Crude oil concentration was measured by gas chromatography (5890A GC system, Hewlett Packard) with a flame ionization detector and Helium as the carrier gas. EPA Method 1663 [44] was used because of the large number of components of crude oil. Accordingly, retention times for the n-alkanes were determined by addition of n-decane, hexadecane, and tetracosane solutions to crude oil samples. Trichlorobenzene (TCB) was used as the internal standard.

Addition technique was used for quantitative analysis. For this purpose, 20  $\mu\text{L}$  of 0.1 % hexadecane solution in dichloromethane (DCM) was added to each sample of crude oil. Extraction procedure was described earlier [45]. Briefly, 1mL of permeate solution was mixed with 1 mL of  $\text{CH}_2\text{Cl}_2$ , 1 mL of saturated NaCl solution (357 g/L), 50  $\mu\text{L}$  of 10mg/mL TCB solution and 5 drops of 1.0 M HCl. After that, 20  $\mu\text{L}$  of 4 % v/v solution of n-decane, 20  $\mu\text{L}$  of 0.5 % v/v solution of hexadecane and 20  $\mu\text{L}$  of 10 mg/mL TCB solution in DCM was added before the injection of the extract. The resulting mixture was

kept for 1 min on a vortex mixer. The organic phase was collected by syringe and kept in a GC vial for further analysis. The injected volume was 1  $\mu\text{L}$  and the injector temperature was 275  $^{\circ}\text{C}$ . The GC oven temperature was programmed to increase from 90 $^{\circ}$  to 250  $^{\circ}\text{C}$  at the rate of 5  $^{\circ}\text{C}/\text{min}$  [44]. The calibration curve for crude oil determination is shown in Figure S1.

## 2.3. Results and Discussion

### 2.3.1 Characteristics of oil-in-water emulsions

#### 2.3.1.1. Droplet's charge and interfacial tension

Interfacial tension of the emulsion and zeta potential of droplets of the dispersed phase are two factors can control droplet coalescence and emulsion stability. Interfacial tension of the oil droplet-solution interface in the presence of 0.001 % v/v CE9500 was measured to be  $21.8 \pm 0.2$  mN/m in synthetic sea water and  $34.9 \pm 0.5$  mN/m in DI water. The noticeable difference between the two values might be the result of change in the hydrophilicity and lipophilicity balance of the surfactant. Previous studies reported that presence of ions can mitigate the interaction of water with the hydrophilic head of surfactant and hence this can make the surfactant more lipophilic (salting out) [19, 46].

The effect of CE9500 on the surface forces was studied before in several studies [8, 11, 47-49]. Gong et al. determined the critical micelle concentration (CMC) of CE9500 to be 22.5 mg/L (0.0024 %v/v) in seawater [50]. The CMC value corresponded to  $\sigma$  of 41.7



mN/m. Venkataraman et al. measured the interfacial tension of Louisiana sweet crude oil in 0.6 M NaCl solution to be  $24.6 \pm 1.1$  mN/m [8]. Powell et al. observed increase in the adsorption of Corexit 9500 to the crude oil-water interface with increasing sea water salinity and reported a reduction in the interfacial tension with addition of salt [11]. A decrease in the interfacial tension was also observed with the increase of CE9500-to-crude oil ratio in 0.6M NaCl solution [8].

Increasing CE9500 concentration decreased the interfacial tension of oil droplet in both DI water and synthetic sea water (Figure 1). Droplet charge was measured to be  $-75.6 \pm 1.6$  mV. CE9500 dispersant is a mixture of anionic and nonionic surfactants. The net negative charge on the droplets is due to the anionic surfactants and, possibly, adsorption of hydroxyl ions [13, 14]. One should expect the charge to be significantly smaller in sea water because of the charge screening effect and a compression of the Debye layer. Thus, the effect of salt on droplet charge counteracts salt-induced changes in the interfacial tension in decreasing the stability of emulsions and promoting droplet coalescence.

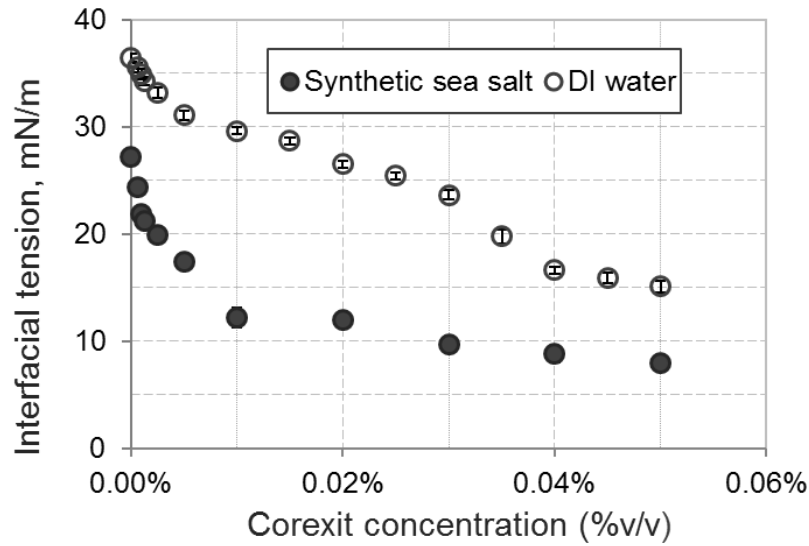


Figure 1.1: The effects of Corexit 9500A on the interfacial tension of crude oil emulsions in deionized water and in synthetic sea water.

Besides, it is known that salt addition can influence the oil droplet charge. In present study, we used synthetic sea salt which consists of mostly mono- and divalent ions ( $\text{Na}^+$ ,  $\text{K}^+$ ,  $\text{Mg}^{2+}$ ,  $\text{Ca}^{2+}$ ,  $\text{Cl}^-$ ,  $\text{SO}_4^{2-}$ ). The effects of mono and divalent ions on droplet's characteristic have been reported in several studies [17, 51]. Tichelkamp et al. measured the interfacial tension of crude oil in the presence of anionic surfactant and revealed that divalent ions are more effective on interfacial tension than monovalent [52]. Gu and Li also reported that divalent and trivalent cations adsorb to oil droplets more readily than monovalent ions [53].

Additionally, due to droplet deformation, it is more complicated to predict stability of droplets. In the condition of high repulsive forces and low IFT, droplet can keep stable. However, change in one or two of these factors can enhance droplet attachment,

deformation and coalescence[54]. In this regard, Binks et al. (2000) reported that the interaction energy which is required for droplet deformation depends on the charge on the drop interfaces and the IFT [51]. In the presence of high salinity, due to decrease in IFT droplet deformations were enhanced and the attraction between the droplets became significant which led to droplets coalescence.

#### 2.3.1.2. Droplet size distribution

Droplet size distributions (DSD) of Corexit-stabilized crude oil emulsions under different conditions were measured in a number of earlier studies [11, 15, 47, 48, 55-57]. Oil viscosity, mixing energy and salinity of the continuous phase were identified as factors that affect DSD. Penetration of Corexit 9500 into oil is lower for higher viscosity oils [47]; accordingly, Mukherjee et al. observed smaller droplets in the emulsions of lower viscosity oils ( $d_{32}$  values of 7.5  $\mu\text{m}$  and 22.5  $\mu\text{m}$  for Arabian light crude oil and Llyod heavy crude oil where the same CE9500-to-oil ratio of 1:100) [55]. Higher mixing energy was shown to give smaller size droplets of oil stabilized by CE9500 [15, 47].

Droplet size distribution (measurements showed that Corexit-stabilized crude oil emulsion in sea water is dominated by small droplets. DSD data for the crude oil and CE9500 dispersed in DI water were recorded as a reference. In synthetic sea water large droplet range narrower than DI water condition. Approximately 96% (by number) of droplets in both emulsions were smaller than 1  $\mu\text{m}$ . Yet, crude oil droplets in DI water were smaller than in synthetic sea water with the mean diameters of 0.59  $\mu\text{m}$  and 0.70

$\mu\text{m}$ , respectively. The difference probably arises from the compression of the electrostatic double layer which promotes the electrostatic attraction between droplets.

Droplet size is another important factor for droplet stability. It is known that small droplets are more stable to coalescence. Yet, under the effects of electrostatic attraction or IFT, they can deform.

Coalescence occur when the liquid film between two adjacent droplets thins and ruptures, and then droplets merge [18]. This process is promoted once droplet charge was shielded by the ionic strength of the emulsion. Previous studies also observed increase in droplet size in the presence of salt [58, 59]. Kundu et al. reported that in the presence of salt, the electrostatic repulsion between droplets decrease due to the reduction of surface charge and hence the droplets coalescence increases [58].

On the other hand, Powell et al. stated that the influence of IFT is more dominant on droplet stabilization [18]. Presence of surfactant which decreases the IFT overshadowed the effects of electrostatic attraction. All in all, in our study, based on number fraction (%) of droplets, electrostatic forces seemed more dominant compare to IFT. However, volume fraction (%) of droplets showed that IFT of oil-aqueous solution is significant, once oil droplet getting larger.

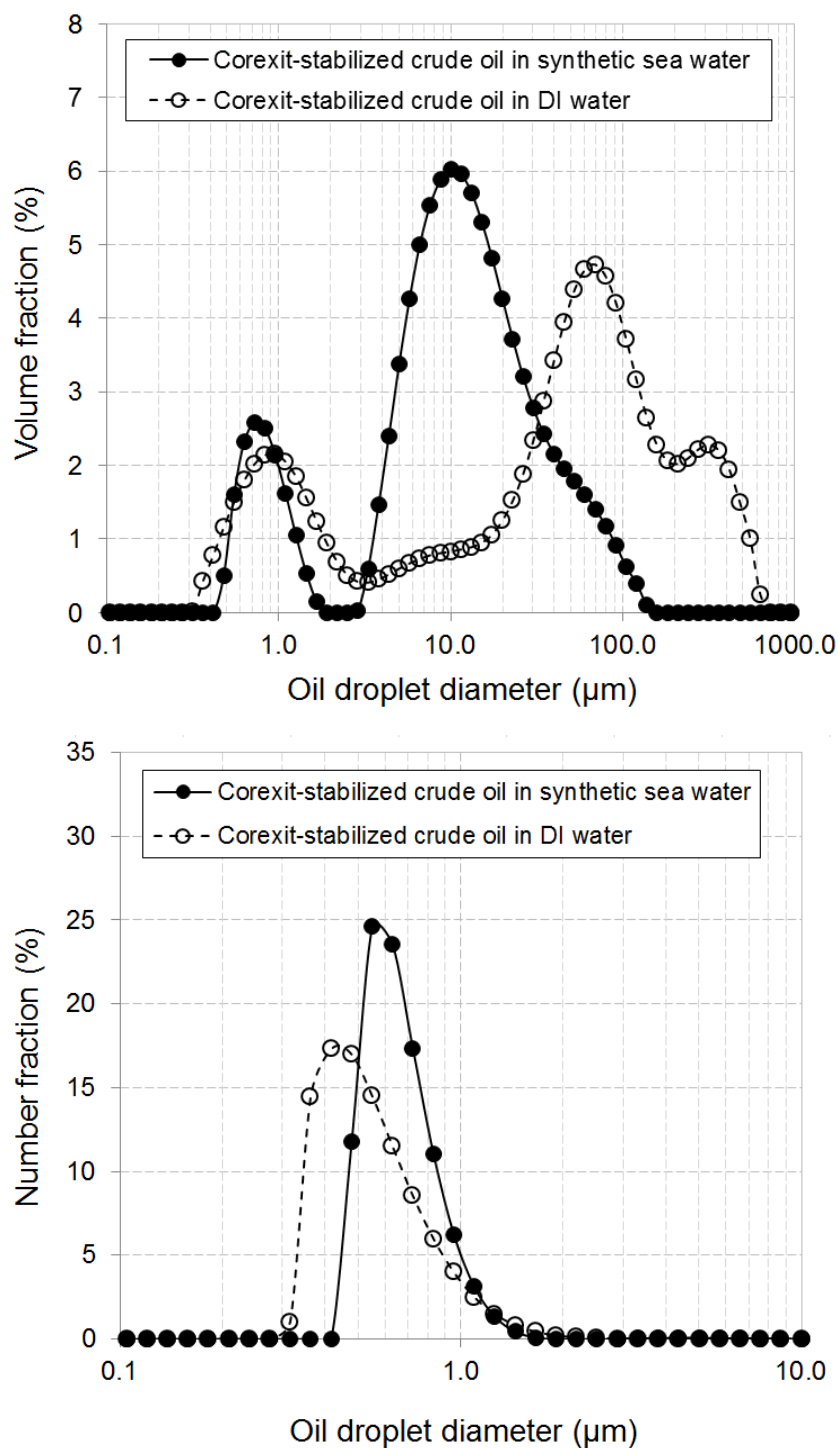


Figure 1.2: Volume-based (a) and number-based (b) droplet size distributions of Corexit-stabilized crude oil emulsions, 1000-10-0 and 1000-10-10, in synthetic sea water and deionized water. The concentration of the oil and the CE9500 dispersant are 1000  $\mu\text{L}(\text{oil})/\text{L}$  and 10  $\mu\text{L}(\text{CE9500})/\text{L}$ . The same emulsions were used in constant pressure microfiltration tests.

## 2.3.2 Membrane selection and characterization

### 2.3.2.1. Hydrophilicity and oleophobicity

The value of the contact angle on a surface varies depending on characteristics of the three phases in contact [60]. A water contact angle, on a membrane surface is often used to estimate membrane hydrophilicity. More hydrophilic surfaces are generally more resistant to fouling [61, 62].

In this study, contact angles of air and crude oil on the 0.4  $\mu\text{m}$  pore size track-etched membrane were measured. Air bubble contact angle on the membrane submerged to DI water was  $153.4^\circ \pm 1.0^\circ$  indicating that the membrane was hydrophilic. In the presence of 0.0010 % (v/v) Corexit 9500A, the contact angles were measured to be  $162.2^\circ \pm 2.3^\circ$  and  $149.6^\circ \pm 0.3^\circ$  in DI and synthetic sea water, respectively. These results showed that membrane hydrophilicity increased with the addition of CE9500 and decreased with an increase in salinity of the solution. An increase in membrane hydrophilicity with the addition of surfactant was reported earlier [61-63]. Pichot et al. [63] observed increase in the contact angle of oil with increasing surfactant concentration until a critical concentration. Chew et al. addressed the hydrophobic interaction between the membrane surface and the hydrophobic tail of surfactant for increasing hydrophilicity [62].

In DI water, the contact angle of crude oil droplets in the presence of CE9500 was  $134.5^\circ \pm 1.1^\circ$  indicating the membrane is oleophobic. In synthetic sea water, the value for

contact angle increased to  $149.4^\circ \pm 0.1^\circ$ . Thus, the salinity of the continuous phase made the membrane less hydrophilic and more oleophobic at the same time. This difference between air bubble and oil droplet contact angle might arise from the result of higher surfactant adsorption on the oil surface or electrostatic repulsion between droplet and oil surface.

Table 2 : Contact angles of air and crude oil with the PVP-coated PCTE membrane in different solutions.

# Aqueous concentration of Corexit 9500A is 0.0010 % (v/v)

Bubble/droplet	Continuous phase		
	DI water	Corexit <sup>#</sup> in DI water	Corexit <sup>#</sup> in sea water
Air bubble	$153.4^\circ \pm 1.0^\circ$	$162.2^\circ \pm 2.3^\circ$	$149.6^\circ \pm 0.3^\circ$
Crude oil droplet	$144.5^\circ \pm 2.8^\circ$	$134.6^\circ \pm 1.1^\circ$	$149.4^\circ \pm 0.1^\circ$

#### 2.3.2.2. Rationale for membrane selection

Since oil droplets are deformable, they can pass through a membrane pore smaller than oil droplet at a sufficiently high transmembrane pressure. The critical pressure required for an oil droplet of diameter,  $d_{drop}$ , to enter a circular pore of diameter,  $d_{pore}$ , is given by eq. (1) [64]:

$$\Delta P_{\text{crit}} = 4\sigma \frac{\cos \theta}{d_{\text{pore}}} \left[ 1 - \left( \frac{2 + 3 \cos \theta - \cos^3 \theta}{4 \left( \frac{d_{\text{drop}}}{d_{\text{pore}}} \right)^3 \cos^3 \theta - (2 - 3 \sin \theta + \sin^3 \theta)} \right)^{1/3} \right] \quad (1)$$

where  $\sigma$  is the interfacial tension and  $\theta = 180^\circ - \varphi$  where  $\varphi$  is the contact angle between the surface of the membrane and the oil droplet at the oil/water interface. Eq. (1) is valid for a single non-wetting droplet pinned at an entry to a single membrane pore.



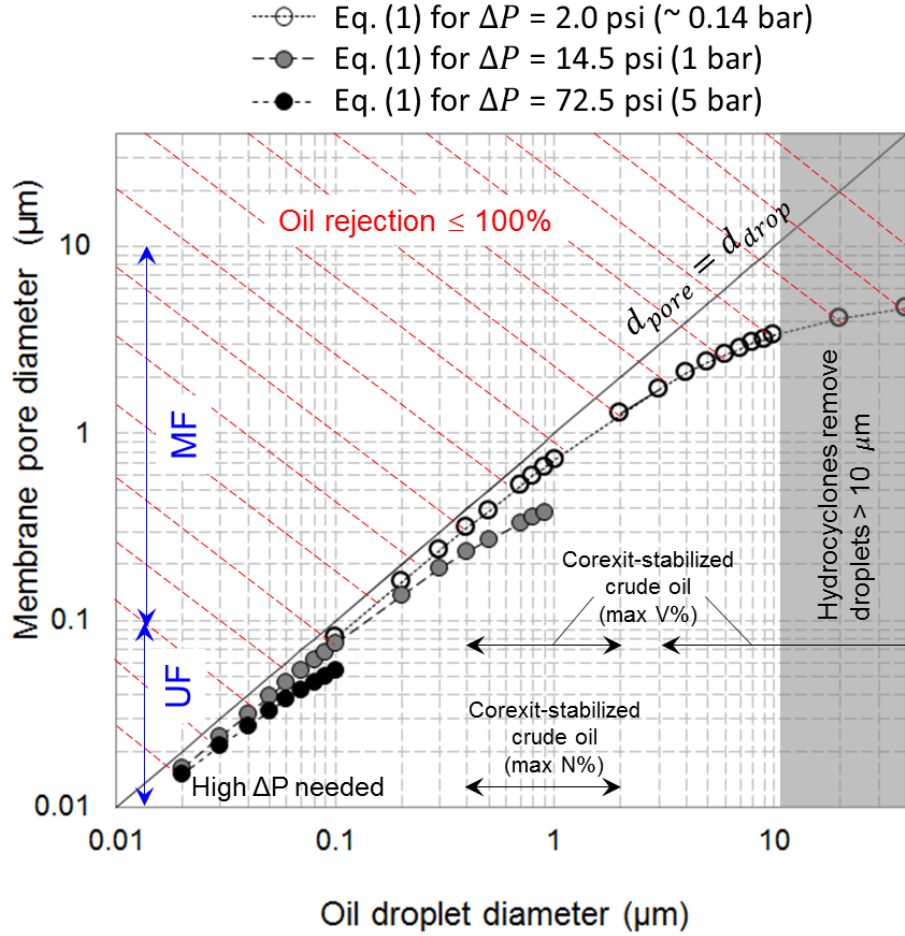


Figure 1.3: Critical transmembrane pressure required as a function of oil droplet size. Critical pressure is the pressure required for a droplet to enter a membrane pore. The calculation is based on eq. (1) and is for crude oil and a membrane with the nominal pore size of  $0.40\ \mu\text{m}$ , interfacial tension,  $\sigma$ , of  $21.84 \pm 0.2\ \text{mN/m}$  (in sea water) and the contact angle  $\phi$ , of  $149.4^\circ \pm 0.1^\circ$  (in sea water).

Figure 3 presents the dependence of the critical pressure as a function of oil droplet size (eq. (1)). The shaded grey zone corresponds to the droplet size domain where droplets can be removed with high efficiency by deoiling hydrocyclones. The domain hashed with red lines corresponds to low oil rejection. The horizontal arrows mark droplet sizes measured for the crude oil used in this study. The vertical arrows denote pore size ranges of membranes categorized as ultra- and microfilters. When searching

for the optimal membrane to remove the emulsified crude oil, we selected microfilters with the pore size of 0.40  $\mu\text{m}$ ; this pore size was close to the maximum possible to allow filtration at the applied transmembrane pressure of 2 psi without oil droplets entering the pores.

### 2.3.3 Assessing filterability of crude oil emulsions

Dead-end microfiltration experiments were performed with PTCE membrane operated at 2 psi constant transmembrane pressure. A clean water flux test and then membrane conditioning with the DI water and synthetic sea water in the presence of 0.001% v/v CE9500 were completed before each oil filtration experiments. During the conditioning of the membrane, the permeate flux was approximately constant.

#### 2.3.3.1 Effect of Corexit 9500A on membrane hydrophilicity/oleophobicity

Conditioning of the membrane with CE9500 solution decreased water contact angle on the membrane surface. Contact angle measurements of air bubble in DI water and CE9500 solution in DI water also verified the increase in hydrophilicity (Table 1). The increase in hydrophilicity led to a higher permeate flux of the Corexit solution  $1714 \pm 147 \text{ L}/(\text{m}^2 \cdot \text{h})$  than the clean water flux  $1500 \pm 103 \text{ L}/(\text{m}^2 \cdot \text{h})$  under the same conditions. In addition, more fouling by oil was observed in filtration experiments performed without prior membrane conditioning with CE9500. However, in the presence of salt in CE9500 solutions slightly decreased the hydrophilicity. The decrease in the hydrophilicity might

arise from the adsorption of the inorganic ions on the membrane surface and a concomitant displacement of the non-ionic surfactants [65].

#### 2.3.3.2 Oil rejection by the membranes

In the present study, this equation was used to determine the critical droplet size for the transmembrane pressure of 2 psi, the value used in microfiltration tests. The critical droplet size was 0.61  $\mu\text{m}$  and 0.52  $\mu\text{m}$  for crude oil emulsified in DI water and synthetic sea water, respectively. Based on the critical droplet size and recorded DSDs, the rejections of oil by the membrane were estimated to be ~94.3% of crude oil in DI water and ~97.8% of crude oil in synthetic sea water. The estimates were of the same order of magnitude but lower than the experimentally determined rejections (99.8% in DI water and 99.7% in synthetic sea water). The higher rejections observed in filtration tests were likely due to the accumulation of oil on the membrane surface. The model described by eq. (1) is for a single non-wetting droplet pinned at an entry to a single membrane pore. However, oil droplets deposit on the membrane surface during filtration. Oil deposition can increase the attraction of a droplet to adjacent droplets leading to droplet coalescence and possible formation of an oil film. Both of these scenarios should lead to rejection values higher than predicted by eq. (1).

### 2.3.3.3 Membrane fouling by Corexit 9500A-stabilized crude oil

The average initial flux of the three replicate filtration experiments with oil emulsions in DI water was  $1719 \pm 16 \text{ L}\cdot\text{m}^2\cdot\text{h}^{-1}$ . The flux declined sharply after the filtration test started. The steady state permeate flux of  $2 \pm 0.5 \text{ L}/(\text{m}^2\cdot\text{h})$  was reached after  $\sim 30$  min (Figure 4b). The average initial flux of the emulsion in synthetic sea water was  $1500 \pm 103 \text{ L}/(\text{m}^2\cdot\text{h})$ . A sharp decline was also observed to the steady state flux of  $18 \pm 3 \text{ L}/(\text{m}^2\cdot\text{h})$  after  $\sim 45$  min (Figure 4a).

The  $\sim 9$  times higher flux in tests with oil suspended in synthetic sea water can be rationalized as resulting from one or a combination of the following effects:

1. Higher contact angle between crude oil droplets and the membrane in synthetic sea water. The higher contact angle means lower surface area is covered by each droplet and a lower number of pores covered by oil and unavailable for permeate flow.
2. Enhanced coalescence of oil droplets in synthetic sea water (Figure 2). The coalescence is promoted by a decrease in the droplet charge due to sorption of divalent cations (lower  $\zeta$ ), screening of electrostatic repulsion at higher ionic strengths (lower Debye length,  $\kappa^{-1}$ ) and lower droplet-membrane affinity (higher  $\theta$ ). Coalesced larger droplets with the same contact angle cover less area than smaller volume of the same total volume. In addition, droplets larger than a critical droplet size are removed by buoyancy and shear forces [42].

3. Lower interfacial tension of oil in the saline solution. If some of the permeation flow occurs by the percolation of water through the oil film, the lower  $\sigma$  should facilitate percolation leading to a higher permeate flux.

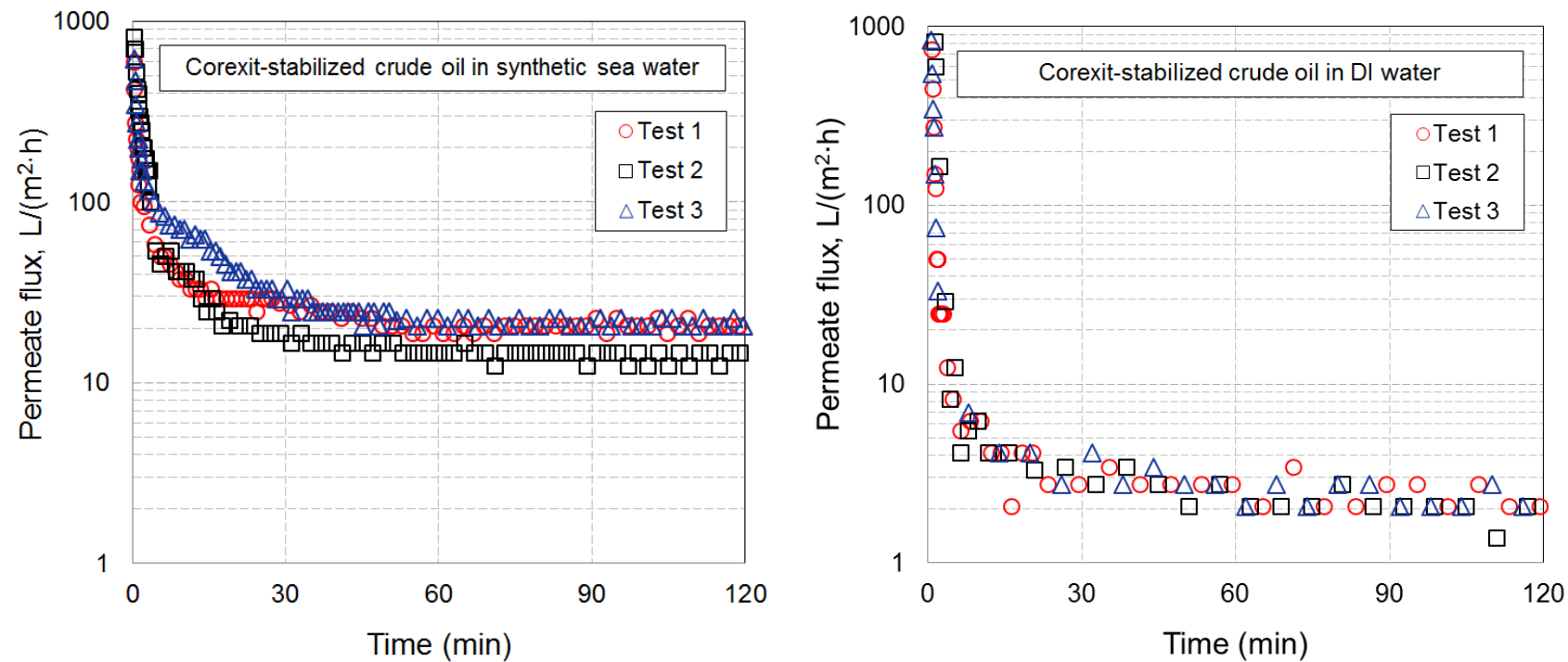


Figure 1.4: Permeate flux behavior in dead-end microfiltration tests with Corexit-stabilized crude oil emulsions. The experiments were performed in a constant pressure regime ( $\Delta P = 2$  psi). The hydraulic resistance of clean membranes averaged over the six tests was  $(31 \pm 2) \cdot 10^9 \text{ m}^{-1}$ .

#### 2.3.3.4 Effect of salinity on permeate flux

Several studies have explored the effect of salt concentration on membrane fouling by emulsified oil [13, 16, 66, 67]. He et al. investigated the fouling of a poly(vinylidene fluoride) microfiltration membrane when challenged with a crude oil-in-water emulsion stabilized by a non-ionic surfactant (Triton X-100) in the presence and absence of salt (NaCl). Derjaguin-Landau-Verwey-Overbeek (DLVO) modeling was used to estimate membrane-oil droplet and oil layer-oil droplet surface interactions [13]. Constant permeate flux crossflow fouling tests revealed more extensive fouling at higher salt concentrations, consistent with DLVO predictions that fouling propensity increases as salt concentration increases. In another study, Zhu et al. examined the fouling of UF membrane using hexadecane-in-water emulsions stabilized by a cationic surfactant (cetyltrimethylammonium bromide; CTAB) and an anionic surfactant (sodium dodecylbenzenesulfonate; DDBS). Flux step filtration of DDBS stabilized emulsions revealed that the addition of 10 mM NaCl did not have a dramatic effect on membrane fouling at low fluxes [16]. However, at high fluxes, the membrane was rapidly fouled due to the screening of repulsive forces between neighboring oil droplets. Unlike the DDBS stabilized emulsion, at low fluxes, the initial rapid fouling disappeared when NaCl was added to the CTAB suspension due to the reduction in electrostatic attraction between the positively charged surfactant and the negatively charged polysulfone UF membrane. At higher fluxes, rapid fouling was still observed. Tanudjaja et al. also reported that critical flux decreased as the salt concentration increased [66]. The addition of salt increased the buoyancy of oil droplets and in turns their tendency to deposit on the

membrane surface along with the screening of the electrostatic repulsion between oil droplets.

#### 2.3.3.5 Microscopy of Corexit-stabilized crude oil emulsions

Athas et al. used an inverted microscope to obtain bright-field images of crude oil-in-water emulsion stabilized by Corexit 9500 A and suspended in seawater [68]. The Corexit 9500 A weigh ratio relative to crude oil was 1:10. Time-lapse microscopic images reveal that the emulsion was initially stable, but rapidly destabilizes and oil droplets coalesce to form an oil rich layer. Within 12 seconds, the focus area was covered with a huge blob. Similar results were also obtained when the Corexit factor was increased by a factor of 10.

#### 2.3.4 DOTM Tests

##### 2.3.4.1 Oil droplet behavior on UF membrane

DOTM test 1 employed the 0.03  $\mu\text{m}$  PCTE membrane and the 100-10-0 emulsion. Most droplet-membrane collisions did not lead to attachment events and only a few oil droplets attached to this UF membrane. Moreover, most coalescence events occurred between a droplet pinned to the membrane surface and another droplet passing by in the crossflow. As the test continued, 35 min into the test, two droplets that were attached to the membrane surface coalesce and form a large film (Figure 5.D). After 64 min, a survey of the membrane was conducted revealing a few large oil films, large



spherical oil droplets that may have resulted from coalescence, and areas of oil-free membrane. A distinct behavior was observed for large spherical droplets and films, where water could still permeate the membrane via these films and droplets (video S1).

DOTM test 2 employed 0.03  $\mu\text{m}$  PCTE membrane and the 100-10-IO emulsion. The only difference between Test 1 and Test 2 is the presence of salt. DOTM Test 2 revealed accumulation of the oil film on the membrane surface despite the relatively low interfacial tension of the emulsion ( $\sigma = 12.2 \text{ mN/m}$ ). Faster oil accumulation was observed with an earlier onset for coalescence and the formation of contiguous oil films as features that set Test 2 apart from Test 1. Video S2 (DOTM Test 2, taken 0 min into the test) shows that the oil film grew much faster than in DOTM Test 1 (Video S1, taken 34 min into the test), which could be attributed to the difference in droplet-droplet interactions in these emulsions. In DOTM Test 1, the membrane became partially covered with an oil film after 35 min; whereas the membrane in DOTM Test 2 was completely covered with an oil film after only 13 min (Figure 5.H). After 60 min, a survey of the membrane showed that the majority of the membrane was covered with large surface area contiguous oil films and with deformed oil droplets so that barely any membrane surface remained oil-free.

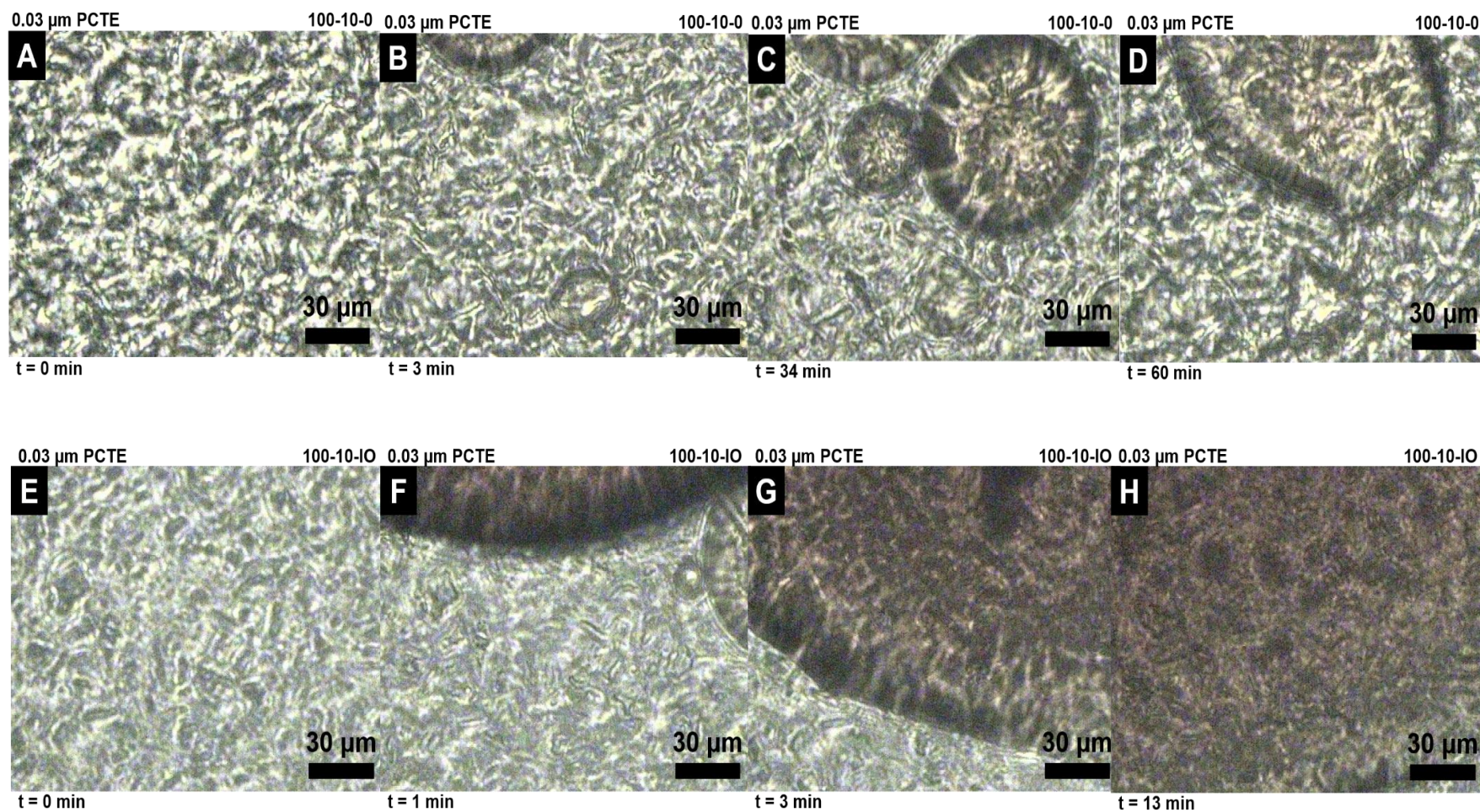


Figure 1.5: Transient behavior of Corexit 9500-stabilized crude oil droplets at the surface of 0.03 μm pore size membrane in DI water (A – D) and in synthetic sea water (E – H). Images A and E correspond to  $t = 0$  when the membrane is unfolded. The direction of crossflow (0.1. m/s) is from left to right in all DOTM images



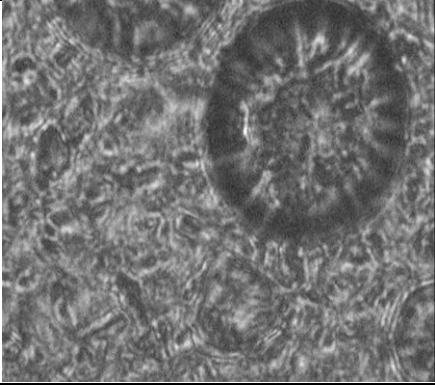
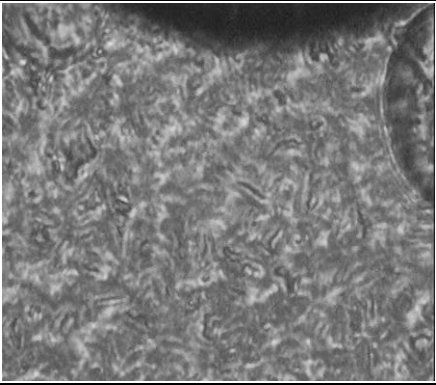
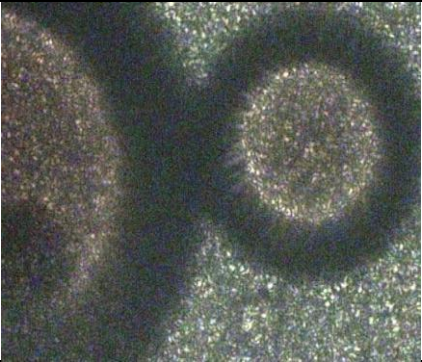
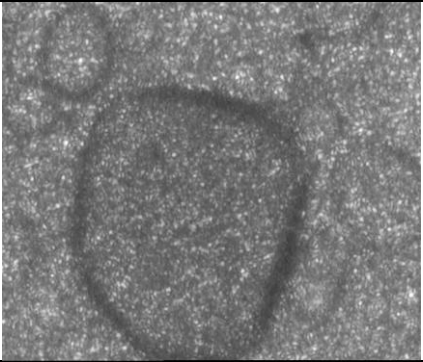
	
<p>Video 1.DOTM Test 1 with 100-10-0 emulsion and 0.03 <math>\mu\text{m}</math> PCTE membrane. The recording starts ~34 min into the test. An oil droplet attaches to the upper right section of the focus area. The droplet has internal movement, which could be attributed to water being trapped inside. This droplet can be seen coalescing in the focus area ~3 min into the video.</p>	<p>Video 2.DOTM Test 2 with 100-10-IO emulsion and 0.03 <math>\mu\text{m}</math> PCTE membrane. The recording starts at the beginning of the experiment. An oil film and large oil droplet can be seen coalescing ~2 min into the video. The oil film grows at a fast rate to cover most of the focus area.</p>
	
<p>Video 3. DOTM Test 3 with 100-10-0 emulsion and 0.2 <math>\mu\text{m}</math> PCTE membrane. The recording starts ~62 min into the experiment. Survey of the membrane surface shows less oil coverage and fouling than in the test with 0.03 <math>\mu\text{m}</math> PCTE membrane (DOTM Test 1).</p>	<p>Video 4.DOTM Test 4 with 100-10-IO emulsion and 0.2 <math>\mu\text{m}</math> PCTE membrane. The recording starts ~66 min into the experiment. Survey of the membrane surface shows deformed oil droplets, oil films, and a few small spherical-shaped droplets.</p>

Figure 1.6: Behavior of Corexit 9500-stabilized crude oil droplets at the surfaces of 0.03  $\mu\text{m}$  and 0.2  $\mu\text{m}$  pore size membranes in DI water and in synthetic sea water

#### 2.3.4.2 Oil droplet behavior on MF membrane

DOTM Test 3 employed the 0.2  $\mu\text{m}$  PCTE membrane and the 100-10-0 emulsion.

Similar to Test 1, most droplets were seen flowing along the membrane surface, in the direction of crossflow, with few attachment events observed (Figure 6). Droplet coalescence on the membrane surface was not observed due to the unfavorable droplet-droplet interactions, which could explain the large portions of the membrane remaining oil-free. The membrane surveyed 62 min into the DOTM test was partly covered by clusters of small oil droplets, large oil droplets that may have resulted from coalescence, and some oil-free areas (Video S3). The membrane surface was relatively less fouled by oil compared to DOTM Test 1.

DOTM test 4 employed the 0.2  $\mu\text{m}$  PCTE membrane and the 100-10-IO emulsion. The presence of salt in DOTM Test 4 promoted more coalescence on the membrane surface. This was expected due to the screening of electrostatic repulsion between oil droplets due to the compression of the Debye layer at the high ionic strength as described earlier. This is consistent with our results with saline model emulsions, where the addition of  $\text{MgSO}_4$  had two opposing effects on emulsion stability: lowered interfacial tension and the  $\zeta$ -potential of oil droplets. However, in both cases, the effect of smaller droplet charge overshadowed the impact of lower interfacial tension [17]. Most coalescence events led to the formation of deformed or flattened droplets (Figure 6.G). Therefore, the effect of crossflow drag force was minimal and the adhesive force was strong between the oil droplets and the membrane surface.

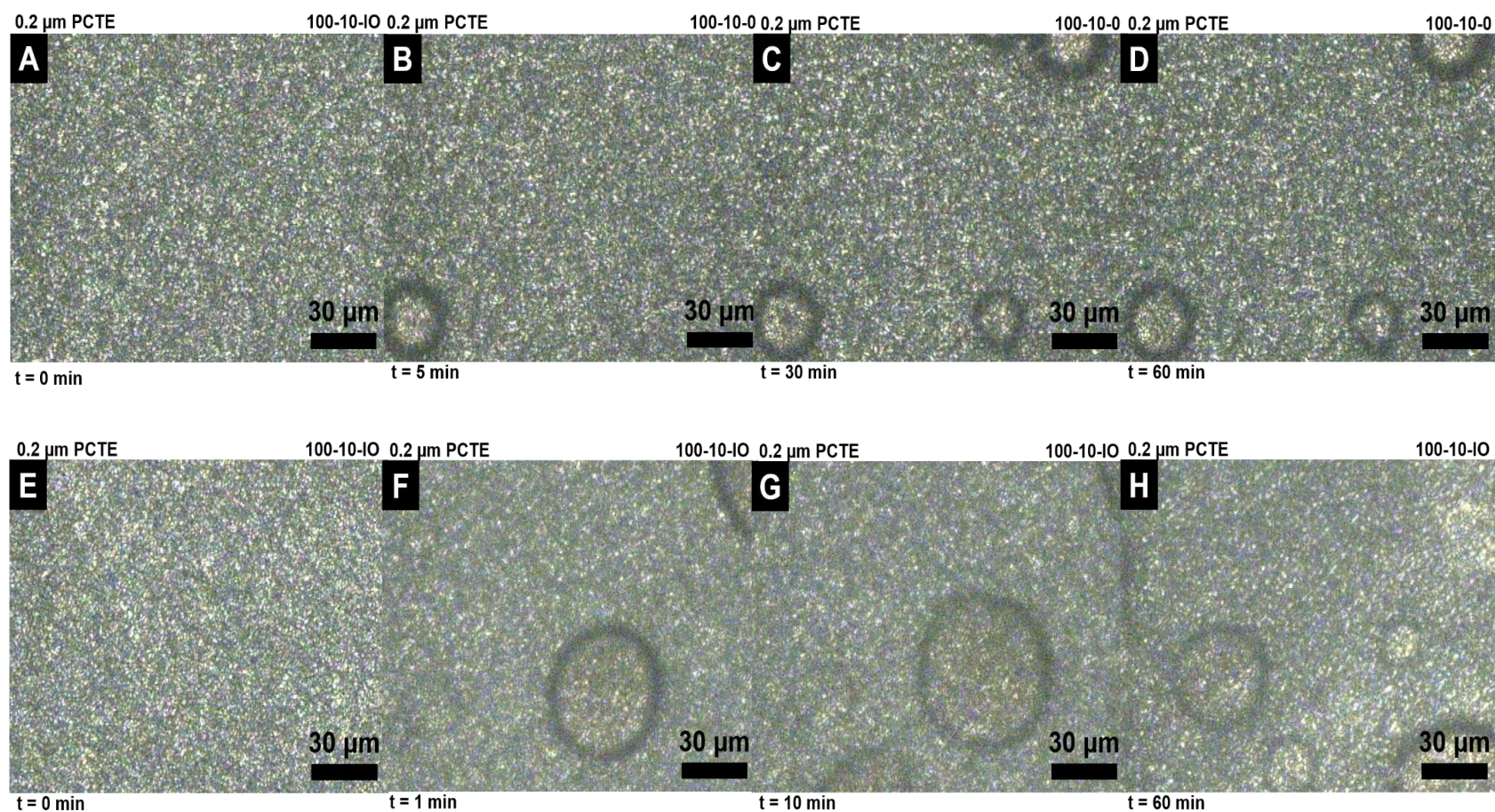


Figure 1.7: Transient behavior of Corexit 9500-stabilized crude oil droplets at the surface of 0.2 μm pore size membrane in DI water (A – D) and in synthetic sea water (E – H). Images A and E correspond to  $t = 0$  when the membrane is unfouled. The direction of crossflow (0.1. m/s) is from left to right in all DOTM images.



## 2.4. Conclusions

Filtration behavior of Corexit 9500 stabilized crude oil emulsions in synthetic sea water was investigated. The emulsion was dominated by sub-micron droplets that carried strong negative charge attributable to the anionic surfactants present in CE9500 and possibly due to adsorption of hydroxyl ions enhanced by nonionic surfactants that partly make up the dispersant. Track etch polycarbonate membranes hydrophilized by PVP were chosen to investigate filterability of the emulsions. The narrow pore distributions of track etch membrane helps ascertain minimal oil permeation and focus on mechanism of membrane fouling. Corexit was found to increase hydrophilicity and oleophilicity of the membranes in DI water but the effects were overcompensated in synthetic sea water. Emulsion characterization and constant pressure stirred dead-end filtration tests revealed that salinity affects the stability of emulsions and can enhance microfiltration performance. Almost complete rejection of oil was achieved but was accompanied by a precipitous flux decline. The low values of the steady state permeate flux indicate that microfiltration is suitable as a polishing step that follows an extensive pretreatment by large throughput deoiling unit processes such as hydrocyclonic separation or flotation. A separate set of Direct Observation Through Membrane (DOTM) tests revealed a complex salinity-dependent behavior of crude oil droplets at the membrane surface. The higher salinity emulsions that showed an order of magnitude higher permeate flux in dead-end microfiltration tests exhibited more coalescence at the membrane surface. This observation pointed to the possibility of water percolation through a lower interfacial tension oil film as a potential mechanism of water permeation through the

fouled membrane. Further studies with phase inversion membranes are warranted to validate result of the present study and evaluate practical limits on permeate flux and oil rejection with high flux ultra- and microfiltration membranes.

## APPENDICES



## APPENDIX A

Calibration curve for oil measurements

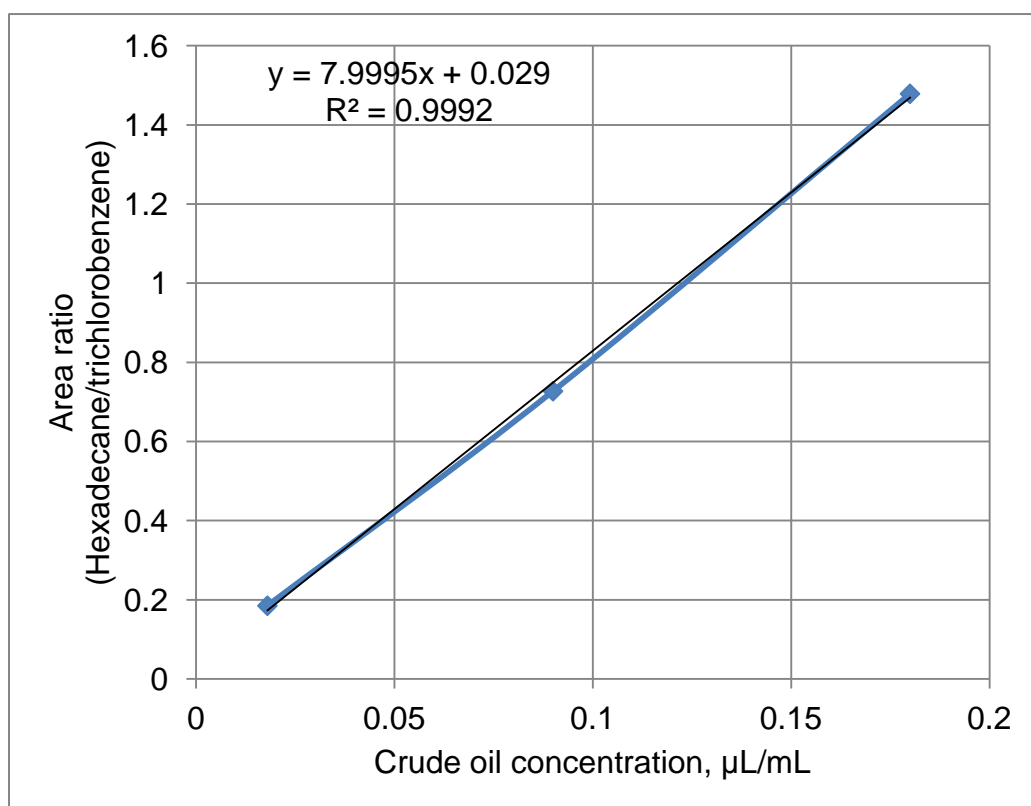


Figure A.1: Calibration curve for crude oil concentration determination.

## APPENDIX B

### Additional filtration tests

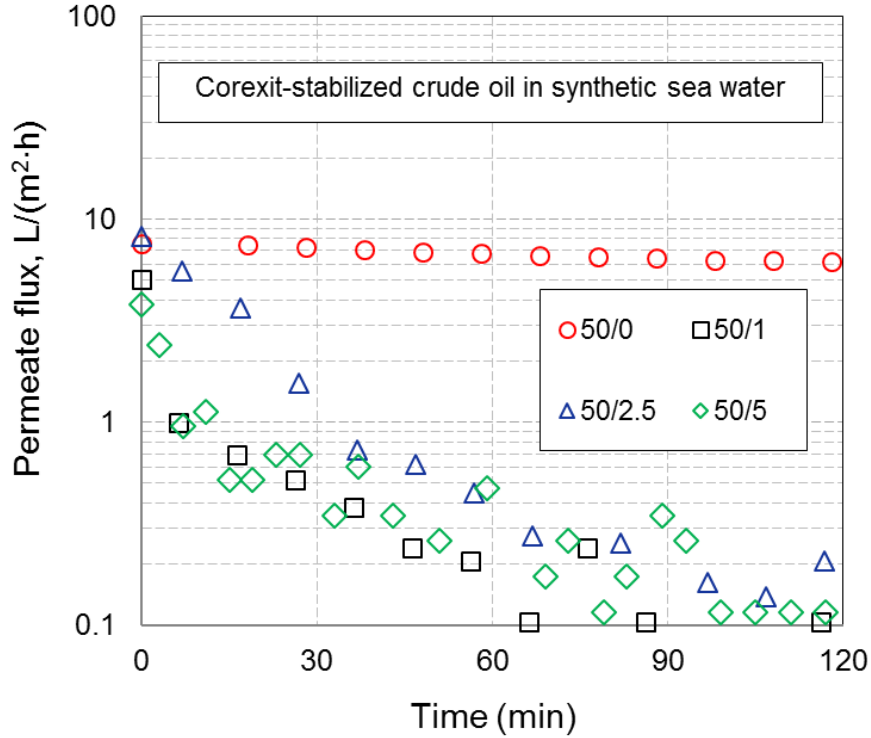


Figure B 1: Permeate flux behavior in dead-end microfiltration tests with Corexit 9500-stabilized crude oil emulsions. Crude oil concentrations were 50 $\mu$ L/L and in the presence of model sea salt. Corexit concentration are 5 (50/5), 2.5 (50/2.5), 1 (50/1)  $\mu$ L/L and absence of Corexit 9500 (50/0). The experiments were performed in a constant pressure regime ( $\Delta P = 8$  psi). The hydraulic resistance of clean membranes averaged was  $3.6 \times 10^{13} \text{ m}^{-1}$ .

## APPENDIX C

### Calculation of the Kolmogorov length scale

The size of the smallest eddy in a turbulent flow named Kolmogorov length scale,  $\eta$ , and is given by:

$$\eta = \left( \frac{\nu^3}{\varepsilon} \right)^{1/4}$$

where  $\eta$  (m) is the size of smallest eddy,  $\nu$  (m<sup>2</sup>/s) is the kinematic viscosity of the fluid and  $\varepsilon$  (J/kg.s) is the average energy dissipation rate of turbulence kinetic energy per unit mass of fluid.

The following values were used as inputs at 20°C:

- Impeller diameter,  $D = 0.05$  m
- Density of the emulsion,  $\rho = 998$  kg/m<sup>3</sup> (approximated by that of water)
- Viscosity of the emulsion,  $\mu = 10.03 \cdot 10^{-4}$  kg/m/s (approximated by that of water)
- Emulsion volume,  $V = 1$  L
- Impeller constant,  $K_T = 1.26$  (value for a pitched-blade turbine (45°) with 4 blades)
- Rotational speed,  $n = 1000$  rpm
- Mixing time,  $t = 1200$  s

The calculated values are:

- Reynolds number for the impeller:  $N_{Re} = D^2 n \rho / \mu = 41459$
- Mixing power:  $P = K_T n^3 D^5 \rho = 1.82$  J/s (W)
- Mean velocity gradient:  $\bar{G} = \sqrt{P / (\mu \cdot V)} = 1347$  s<sup>-1</sup>
- Energy dissipation rate:  $\varepsilon = P / (\rho \cdot V) = 1.82$  W/kg
- Kolmogorov length scale:  $\eta = (\mu^3 / (\rho^3 \cdot \varepsilon))^{1/4} = 27.3$   $\mu$ m

## REFERENCES

## REFERENCES

- [1] M.K. McNutt, R. Camilli, T.J. Crone, G.D. Guthrie, P.A. Hsieh, T.B. Ryerson, O. Savas, F. Shaffer, Review of flow rate estimates of the Deepwater Horizon oil spill, *PNAS*, 109 (2012) 20260-20267.
- [2] D. Wolf, Ecological Impacts of Deepwater Horizon Oil Spill (Bogota, Columbia), in, 2012.
- [3] D.L. Valentine, I. Mezić, S. Maćešić, N. Črnjarić-Žić, S. Ivić, P.J. Hogan, V.A. Fonoberov, S. Loire, Dynamic autoinoculation and the microbial ecology of a deep water hydrocarbon irruption, *PNAS*, 109 (2012) 20286.
- [4] T. Federal Interagency Solutions Group, Oil budget calculator deepwater Horizon, 2011.
- [5] B. Place, B. Anderson, A. Mekebri, E.T. Furlong, J.L. Gray, R. Tjeerdema, J. Field, A role for analytical chemistry in advancing our understanding of the occurrence, fate, and effects of Corexit oil dispersants, *Environ. Sci. Technol.*, 44 (2010) 6016-6018.
- [6] K.A. Burns, R. Jones, Assessment of sediment hydrocarbon contamination from the 2009 Montara oil blow out in the Timor Sea, *Environ. Pollut.*, 211 (2016) 214-225.
- [7] B.J. Place, M.J. Perkins, E. Sinclair, A.L. Barsamian, Trace analysis of surfactants in Corexit oil dispersant formulations and seawater, *Deep Sea Res. II*, 129 (2016) 273-281.
- [8] P. Venkataraman, J. Tang, E. Frenkel, G.L. McPherson, J. He, S.R. Raghavan, V. Kolesnichenko, A. Bose, V.T. John, Attachment of a hydrophobically modified biopolymer at the oil–water interface in the treatment of oil spills, *ACS Appl. Mater. Inter.*, 5 (2013) 3572-3580.
- [9] A. George-Ares, J.R. Clark, Aquatic toxicity of two Corexit® dispersants, 40 (2000) 897-906.
- [10] P. Walstra, Principles of emulsion formation, *Chem. Eng. Sci.*, 48 (1993) 333-349.
- [11] K.C. Powell, A. Chauhan, Dynamic interfacial tension and dilational rheology of dispersant Corexit 9500, *Colloid Surface A*, 497 (2016) 352-361.
- [12] J.C. Berg, *An Introduction to Interfaces and Colloids The Bridge to Nanoscience*, World Scientific Publishing Co., 2012.

- [13] Z. He, S. Kasemset, A.Y. Kirschner, Y.-H. Cheng, D.R. Paul, B.D. Freeman, The effects of salt concentration and foulant surface charge on hydrocarbon fouling of a poly(vinylidene fluoride) microfiltration membrane, *Water Res.*, 117 (2017) 230-241.
- [14] K.G. Marinova, R.G. Alargova, N.D. Denkov, O.D. Velev, D.N. Petsev, I.B. Ivanov, R.P. Borwankar, Charging of oil–water interfaces due to spontaneous adsorption of hydroxyl ions, *Langmuir*, 12 (1996) 2045-2051.
- [15] M.C. Sterling, J.S. Bonner, A.N.S. Ernest, C.A. Page, R.L. Autenrieth, Chemical dispersant effectiveness testing: influence of droplet coalescence, *Mar. Pollut. Bull.*, 48 (2004) 969-977.
- [16] X. Zhu, A. Dudchenko, X. Gu, D. Jassby, Surfactant-stabilized oil separation from water using ultrafiltration and nanofiltration, *J. Membr. Sci.*, 529 (2017) 159-169.
- [17] E.N. Tummons, J.W. Chew, A.G. Fane, V.V. Tarabara, Ultrafiltration of saline oil-in-water emulsions stabilized by an anionic surfactant: Effect of surfactant concentration and divalent counterions, *J. Membr. Sci.*, 537 (2017) 384-395.
- [18] K.C. Powell, R. Damitz, A. Chauhan, Relating emulsion stability to interfacial properties for pharmaceutical emulsions stabilized by Pluronic F68 surfactant, *International Journal of Pharmaceutics*, 521 (2017) 8-18.
- [19] K. Shinoda, H. Takeda, The effect of added salts in water on the hydrophile-lipophile balance of nonionic surfactants: The effect of added salts on the phase inversion temperature of emulsions, *J. Colloid Interface Sci.*, 32 (1970) 642-646.
- [20] G.J. Blondina, M.M. Singer, I. Lee, M.T. Ouano, Influence of salinity on petroleum accommodation by dispersants, *Spill Sci. Technol. Bull.*, 5 (1999) 127-134.
- [21] K.C. Powell, A. Chauhan, Dynamic interfacial tension and dilational rheology of dispersant Corexit 9500, *Colloids and surfaces. A, Physicochemical and engineering aspects*, 497 352-361.
- [22] E.N. Tummons, J.W. Chew, A.G. Fane, V.V. Tarabara, Ultrafiltration of saline oil-in-water emulsions stabilized by an anionic surfactant: Effect of surfactant concentration and divalent counterions, 537 (2017) 384-395.
- [23] E.N. Tummons, V.V. Tarabara, Jia W. Chew, A.G. Fane, Behavior of oil droplets at the membrane surface during crossflow microfiltration of oil–water emulsions, 500 (2016) 211-224.
- [24] Z. Pan, L. Zhao, M.C. Boufadel, T. King, Impact of mixing time and energy on the dispersion effectiveness and droplets size of oil, *Chemosphere (Oxford)*, 166 246-254.

- [25] B.P. Binks, W.G. Cho, P.D.I. Fletcher, D.N. Petsev, Stability of Oil-in-Water Emulsions in a Low Interfacial Tension System, *Langmuir*, 16 (2000) 1025-1034.
- [26] M.C. Sterling, J.S. Bonner, A.N.S. Ernest, C.A. Page, R.L. Autenrieth, Chemical dispersant effectiveness testing: influence of droplet coalescence, 48 (2004) 969-977.
- [27] Z. Li, K. Lee, T. King, H. Niu, Application of entropy analysis of in situ droplet-size spectra in evaluation of oil chemical dispersion efficacy, *Marine Pollution Bulletin*, 62 (2011) 2129-2136.
- [28] A.L. Ahmad, M.A. Majid, B.S. Ooi, Functionalized PSf/SiO<sub>2</sub> nanocomposite membrane for oil-in-water emulsion separation, *Desalination*, 268 (2011) 266-269.
- [29] D. Lu, L. Dongwei, Z. Tao, M. Jun, Ceramic membrane fouling during ultrafiltration of oil/water emulsions: Roles played by stabilization surfactants of oil droplets, *Environ. Sci. Technol.*, 49 (2015) 4235–4244.
- [30] T. Frankiew, Understanding the fundamentals of water treatment. The dirty dozen-12 common causes of poor water quality, in: *Proceedings of the 11. Produced Water Seminar* Houston, TX, 2001.
- [31] M. Cheryan, N. Rajagopalan, Membrane processing of oily streams. Wastewater treatment and waste reduction, *J. Membr. Sci.*, 151 (1998) 13-28.
- [32] S. Lee, Y. Aurelle, H. Roques, Concentration polarization, membrane fouling and cleaning in ultrafiltration of soluble oil, *J. Membr. Sci.*, 19 (1984) 23-38.
- [33] K.J. Milić, A. Murić, I. Petrinić, M. Simonič, Recent developments in membrane treatment of spent cutting-pils: A review, *Ind. Eng. Chem. Res.*, 52 (2013) 7603-7616.
- [34] J. Mueller, Y. Cen, R.H. Davis, Crossflow microfiltration of oily water, 129 (1997) 221-235.
- [35] S. Lee, Y. Aurelle, H. Roques, Concentration polarization, membrane fouling and cleaning in ultrafiltration of soluble oil, 19 (1984) 23-38.
- [36] E. Matthiasson, B. Sivik, Concentration polarization and fouling, 35 (1980) 59-103.
- [37] D. Lu, L. Dongwei, Z. Tao, M. Jun, Ceramic Membrane Fouling during Ultrafiltration of Oil/Water Emulsions: Roles Played by Stabilization Surfactants of Oil Droplets, *Environmental science & technology*, 49.
- [38] B. Chakrabarty, A.K. Ghoshal, M.K. Purkait, Ultrafiltration of stable oil-in-water emulsion by polysulfone membrane, 325 (2008) 427-437.

- [39] X. Zhu, A. Dudchenko, X. Gu, D. Jassby, Surfactant-stabilized oil separation from water using ultrafiltration and nanofiltration, *Journal of membrane science*, 529 159-169.
- [40] G.A.L. Delvigne, C.E. Sweeney, Natural dispersion of oil, *Oil Chem. Pollut.*, 4 (1988) 281-310.
- [41] A.K. George, R.N. Singh, Correlation of refractive index and density of crude oil and liquid hydrocarbon, *Int. J. Chem. Environ. Biol. Sci.*, 3 (2015) 420-422.
- [42] E.N. Tummons, V.V. Tarabara, Jia W. Chew, A.G. Fane, Behavior of oil droplets at the membrane surface during crossflow microfiltration of oil–water emulsions, *J. Membr. Sci.*, 500 (2016) 211-224.
- [43] H. Li, A.G. Fane, H.G.L. Coster, S. Vigneswaran, Direct observation of particle deposition on the membrane surface during crossflow microfiltration, *J. Membr. Sci.*, 149 (1998) 83-97.
- [44] EPA, Methods for the Determination of Diesel, Mineral, and Crude Oils in Offshore Oil and Gas Industry Discharges, in: *Differentiation of Diesel and Crude Oil by GC/FID*, Office of Water Engineering and Analysis Division. Washington DC, 1992.
- [45] Z. Yang, V.V. Tarabara, M.L. Bruening, Adsorption of anionic or cationic surfactants in polyanionic brushes and its effect on brush swelling and fouling resistance during emulsion filtration, *Langmuir*, 31 (2015) 11790-11799.
- [46] Y. Kawashima, T. Hino, H. Takeuchi, T. Niwa, Stabilization of water/oil/water multiple emulsion with hypertonic inner aqueous phase, *Chem. Pharm. Bull.*, 40 (1992) 1240-1246.
- [47] Z. Pan, L. Zhao, M.C. Boufadel, T. King, Impact of mixing time and energy on the dispersion effectiveness and droplets size of oil, *Chemosphere* 166 (2017) 246-254.
- [48] B. Mukherjee, B.A. Wrenn, Effects of physical properties and dispersion conditions on the chemical dispersion of crude oil, *Environ. Eng. Sci.*, 28 (2011) 263-273.
- [49] T.L. King, J.A.C. Clyburne, K. Lee, B.J. Robinson, Interfacial film formation: Influence on oil spreading rates in lab basin tests and dispersant effectiveness testing in a wave tank, *Mar. Pollut. Bull.*, 71 (2013) 83-91.
- [50] Y. Gong, X. Zhao, S.E. O'Reilly, T. Qian, D. Zhao, Effects of oil dispersant and oil on sorption and desorption of phenanthrene with Gulf Coast marine sediments, *Environ. Poll.*, 185 (2014) 240-249.
- [51] B.P. Binks, W.-G. Cho, P.D.I. Fletcher, D.N. Petsev, Stability of oil-in-water emulsions in a low interfacial tension system, *Langmuir*, 16 (2000) 1025-1034.



- [52] T. Tichelkamp, Y. Vu, M. Nourani, G. Øye, Interfacial tension between low salinity solutions of sulfonate surfactants and crude and model oils, *Energy Fuels*, 28 (2014) 2408-2414.
- [53] Y. Gu, D.-D. Li, An electrical suspension method for measuring the electric charge on small silicone oil droplets dispersed in aqueous solutions, *J. Colloid Interface Sci.*, 195 (1997) 343-352.
- [54] D.E. Tambe, M.M. Sharma, Factors controlling the stability of colloid-stabilized emulsions: I. An experimental investigation, *J. Colloid Interface Sci.*, 157 (1993) 244-253.
- [55] B. Mukherjee, B.A. Wrenn, P. Ramachandran, Relationship between size of oil droplet generated during chemical dispersion of crude oil and energy dissipation rate: Dimensionless, scaling, and experimental analysis, *Chem. Eng. Sci.*, 68 (2012) 432-442.
- [56] Z.M. Aman, C.B. Paris, E.F. May, M.L. Johns, D. Lindo-Atichati, High-pressure visual experimental studies of oil-in-water dispersion droplet size, *Chem. Eng. Sci.*, 127 (2015) 392-400.
- [57] P.J. Brandvik, Ø. Johansen, F. Leirvik, U. Farooq, P.S. Daling, Droplet breakup in subsurface oil releases - Part 1: Experimental study of droplet breakup and effectiveness of dispersant injection, *Mar. Pollut. Bull.*, 73 ((2013) 319-326.
- [58] P. Kundu, A. Agrawal, H. Mateen, I.M. Mishra, Stability of oil-in-water macro-emulsion with anionic surfactant: Effect of electrolytes and temperature, *Chem. Eng. Sci.*, 102 (2013) 176-185.
- [59] G. Ríos, C. Pazos, J. Coca, Destabilization of cutting oil emulsions using inorganic salts as coagulants, *Colloid Surface A*, 138 (1998) 383-389.
- [60] V.S. Kulkarni, C. Shaw, Chapter 2 - Surfactants, Lipids, and Surface Chemistry, in, *Academic Press*, Boston, 2016, pp. 5-19.
- [61] A.G. Fane, C.J.D. Fell, K.J. Kim, The effect of surfactant pretreatment on the ultrafiltration of proteins, *Desalination*, 53 (1985) 37-55.
- [62] N.G.P. Chew, S. Zhao, C.H. Loh, N. Permogorov, R. Wang, Surfactant effects on water recovery from produced water via direct-contact membrane distillation, *J. Membr. Sci.*, 528 (2017) 126-134.
- [63] R. Pichot, F. Spyropoulos, I.T. Norton, Competitive adsorption of surfactants and hydrophilic silica particles at the oil–water interface: Interfacial tension and contact angle studies, *J. Colloid Interface Sci.*, 377 (2012) 396-405.

[64] F.F. Nazzal, M.R. Wiesner, Microfiltration of oil-in-water emulsions, *Water Environ. Res.*, 68 (1996) 1187-1191.

[65] R. Denoyel, J. Rouquerol, Thermodynamic (including microcalorimetry) study of the adsorption of nonionic and anionic surfactants onto silica, kaolin, and alumina, *J. Colloid Interface Sci.*, 143 (1991) 555-572.

[66] H.J. Tanudjaja, W. Pee, A.G. Fane, J.W. Chew, Effect of spacer and crossflow velocity on the critical flux of bidisperse suspensions in microfiltration, *J. Membr. Sci.*, 513 (2016) 101-107.

[67] F.L. Hua, Y.F. Tsang, Y.J. Wang, S.Y. Chan, H. Chua, S.N. Sin, Performance study of ceramic microfiltration membrane for oily wastewater treatment, *Chem. Eng. J.*, 128 (2007) 169-175.

[68] J.C. Athas, K. Jun, C. McCafferty, O. Owoseni, V.T. John, S.R. Raghavan, An effective dispersant for oil spills based on food-grade amphiphiles, *Langmuir*, 30 (2014) 9285-9294.

## CHAPTER THREE

Microfiltration of hexadecane emulsions stabilized by sodium dodecyl sulfate surfactant

### 3.1. Introduction

Oily wastewater produces by a number of industries. The concentration and amount of the oil can vary depend on the industries. Oil gas industry is one of the largest oily wastewater source and its main waste stream is produced water which is the water from oil-gas reservoir [1]. Daily large amount of produced water discharged into the sea and its oil concentration usually changes between 50-1000 mg/L [2].

The amount of the oil in produced water poses a risk in aquatic life; especially the rise in offshore oil-gas exploration and production increases this risk. However, it is not the biggest danger on environment. In 1989 Exxon Valdez [3], in 1991 Gulf oil spill and in 2010 Deepwater horizon oil spill (DWH) [4] resulted in huge amount of oil release into the sea. In the case of DWH incident 5 million barrels of oil spill into the Gulf of Mexico which caused higher oil release than produced water for the same period of time with the DWH incident [5]. Thus, the Gulf's habitat was affected harmfully from the oil spill. In order to reduce the effects of the spill dispersants were used. Dispersants are a key appliance to decrease disastrous impact of oil spills. In the DWH case, Corexit 9500A and Corexit 9725 were used [5]. The application of these dispersants enhanced the

break of oil into small droplets which reduced the local concentration of oil and extended the retention time of the oil droplets in the water column [6].

Both produced water and oily wastewater from oil spills have crude oil with in variety of droplet sizes. In the presence of surfactant, oil droplets can be in emulsified formed. In this form, the conventional oil-water separation methods are usually ineffective to remove small oil droplets [7]. However, membranes can offer a very competitive oil treatment. It has high removal efficiency, low capital cost and easy operation [ 7]. Yet, membrane fouling still remains as an obstacle to widespread application of membranes. Studies to understand membrane fouling mechanism revealed several points which can attribute membrane fouling (ionic strength, surfactant to oil ratio and membrane characteristic) [8-13]. Ionic strength is the one of the major factor can control membrane fouling during filtration of oil in water emulsions. Most of the produced water and oily wastewater from oil spill depending on spill point have mostly high ionic strength [14]. The salinity of sea water is roughly 35,000 ppm and the produced water salinity is in the range of 1,000 ppm to 250,000ppm [14]. Thus, understanding the effect of salt on membrane fouling is essential to optimize membrane filtration.

Beside salinity, surfactants are also effective on membrane fouling and it can have associated impact on fouling with salinity [15]. Surfactant molecules adsorbs at the oil-water interface and form a thin interfacial film between water and oil surface which decreases interfacial tension (IFT) between two liquids [16, 17]. Decrease in IFT minimizes the contact, coalescence and aggregation of the oil droplets [18].

Depending on surfactants' hydrophilic head, oil droplets can be charged, and charge creates an electrostatic repulsion between oil droplets [19]. In presence of salt, droplets' charge alters which affects the repulsion forces between oil droplets and it also changes the interaction between oil droplets and membrane surface [11, 12]. He Z. et al. investigated membrane-oil droplet and oil layer-oil droplet surface interaction. The membrane fouling propensity increased with the addition of salt [12]. While, increase in salt concentration reduces the repulsion between negatively charge oil droplets and between oil droplets-oil layer on membrane surface, promotes the membrane fouling. In the earlier stage of filtration, membrane – oil droplets surface interaction is dominant until sufficient oil droplet depositions forms oil layer [20]. Visualization of the membrane surface during filtration clarified the membrane fouling stages. In the earlier stage, droplet attachment and clustering occur on membrane surface. Smaller droplets surround the larger droplet. Following stages, grown droplet clusters press each other until they deform and then continuing deformation result in coalescence [21].

The observation of the membrane surface in the absence of permeate flux revealed that in presence of salt promote the oil droplet coalescence. In the case of permeate flux, droplets' residence time on membrane surface is longer and permeate drag forces allow to more droplet deformation and enhance the droplet coalescence [11].

In Chapter One, CE9500 stabilized crude oil emulsions' microfiltration was investigated in DI and synthetic sea water. The reason of this study is understanding the effect of CE9500 on the characteristic of oil-water emulsions and membrna surface. Crude oil

composition can vary extremely and the exact composition of CE9500 is a property. Therefore, effects of CE9500 are not well known, especially during filtration. Thus, in this study CE9500 stabilized emulsions filterability were investigated in saline and nonsaline conditions. In the absence of salt, sharp permeate flux decline was observed. However, in the presence of synthetic sea salt, less dramatic flux decline was measured. Higher flux in synthetic sea water related to the one or a combination of the following effects. First, bigger contact angle of oil droplet on the membrane surface in synthetic sea water decreased the area which was covered by oil droplets, so less number of pore covered by oil. Second, addition of salt promotes the droplet coalescence and lower droplet-membrane affinity. Third, the percolation of water through the oil film due to lower interfacial tension.

Chapter One showed that salinity is critical factor on membrane fouling, but due to complex compound of crude oil and CE9500, the parameters can attribute the fouling are not well known, so it is not convenient to understand the exact effect of salinity. Thus, in this chapter model emulsions were prepared in different salinities. Hexadecane emulsions were stabilized by anionic surfactant SDS (CE9500 is the mixture of nonionic and anionic surfactants). Droplet size distribution, contact angle measurement were used to characterize the emulsions. Microfiltration experiments were conducted at constant transmembrane pressure by using dead-end filtration cell. Oil rejections were measured by GC.

## 3.2. Materials and Methods

### 3.2.1. Reagents

Hexadecane (HD, 99%), n-decane ( $\geq 99\%$ ), sodium dodecyl sulfate (SDS,  $\geq 98.5\%$ ), magnesium sulfate heptahydrate ( $\text{MgSO}_4 \cdot 7\text{H}_2\text{O}$ ,  $\geq 98\%$ ), sodium chloride (NaCl) were purchased from Sigma-Aldrich. Dichloromethane and potassium chloride (KCl, 99%) were purchased from J.T. Baker. Hydrochloric acid (HCl, EMD Chemicals) was diluted to 1 M. Deionized (DI) water was produced by a Milli-Q ultrapure water system (Integral 10, Millipore) equipped with a terminal 0.2  $\mu\text{m}$  microfilter (MilliPak, Millipore); the water resistivity was  $\sim 18 \text{ M}\Omega \cdot \text{cm}$ .

### 3.2.2 Preparation and characterization of oil-water emulsions

The hexadecane emulsions were prepared in the presence of 0.1mM SDS. The hexadecane content in all emulsions was 0.1% v/v (1000  $\mu\text{L}(\text{HD})/\text{L}$ ). The emulsions were prepared in DI water condition and in different salinities. The salinities of emulsions were 6.7 mM  $\text{MgSO}_4$ , 54.3 mM  $\text{MgSO}_4$ , 469 mM NaCl, model sea water, which involved 54.3mM  $\text{MgSO}_4$  and 469 mM NaCl. The solutions for either conditioning of membrane or contact angle measurements were prepared at the salt concentrations of 6.7 mM  $\text{MgSO}_4$ , 54.3 mM  $\text{MgSO}_4$ , 469 mM NaCl, model sea water and 1 mM SDS concentration was used for all solutions. Both emulsions and solutions were prepared as 1000ml and the oil-water-surfactant mixtures were mixed at 1,000 rpm using a digital stand mixer (RW 20 digital dual range-mixer, IKA) for 20 min.

Light diffraction (Malvern Mastersizer 2000) was used to measure droplet size distributions of the hexadecane emulsions. The refractive index for hexadecane is 1.434. During droplet size measurement, the hexadecane emulsions were circulated from the sample dispersion unit stirred at 1,000 rpm, through the optical cell of the particle sizer and back into the dispersion unit. Instrument's software reported the volume-based distributions and it was converted to the number-based distributions based on the volume-based data.

### 3.2.3 Measurement of hexadecane concentration

Hexadecane concentrations in permeate was measured by gas chromatography (5890A GC system, Hewlett Packard) equipped with a flame ionization detector. Helium was used as the carrier gas. The injected volume was 1  $\mu\text{L}$ . Hexadecane was extracted from permeate with dichloromethane (DCM) [35]. For the extraction, 100  $\mu\text{L}$  of permeate solution was mixed with 1 mL of  $\text{CH}_2\text{Cl}_2$ , 1 mL of saturated NaCl solution (357 g/L), and 5 drops of 1.0 M HCl. After that 30  $\mu\text{L}$  of 0.05 % v/v solution of n-decane in DCM was added as an internal standard (IS). The resulting mixture was mixed for 1 min on a vortex mixer. The organic phase was collected by syringe and kept in GC vial for further analysis.



The injector temperature was set 250 °C. The GC oven temperature was programmed to increase from 100 to 260 °C at the rate of 20 °C/min. The calibration curve for hexadecane determination is shown in Figure S1.

#### 3.2.4 Dead-end microfiltration system

Microfiltration of hexadecane emulsions were conducted at 2 psi constant transmembrane pressure by using a stainless-steel filtration cell (HP 4750, Sterlitech Corp., Kent, WA). A hydrophilic polycarbonate track-etch (PTCE) membrane with a nominal size of 0.40  $\mu\text{m}$  was placed in the cell. During filtration tests, the emulsions were mixed by magnetic stirrer at degree 3 (Corning, PC-510). Permeate mass was continuously recorded by an electronic mass balance (Adventurer Pro AV812, OHAUS Corp.). Clean water flux test and conditioning with aqueous solutions of SDS were recorded before each flux test. Clean membrane's hydraulic resistivity was determined by clean water flux data, which were recorded flux data for different transmembrane pressure (1 psi, 2 psi, 3 psi and 4 psi). Conditioning tests were conducted at 2 psi. During conditioning tests, any flux decline was observed.

#### 3.2.5. Membrane characterization

Contact angle of hexadecane on the membrane surface were determined by the goniometer in DI water. DI water was filled in the standard quartz cell. The membrane was fixed to the environmental fixture (part 100-14, rame-hart instrument co.) with the

feed side facing downward and it was submerged in DI water. The hexadecane droplet was released below the membrane by the inverted stainless steel 22g needle. The contact angle of the droplet in the submerged membrane surface was determined by DROPImage Advanced software based on the shape of droplet.

### 3.3. Results and Discussion

#### 3.3.1 Characteristics of oil-in-water emulsions

The published value of hexadecane-water interfacial tension is 41.8 mN/m. In the presence of 0.1mM SDS, it was measured to be 39.3 mN/m and with the addition of 6.7mM  $\text{MgSO}_4$ , this value decreased to 21.7 mN/m [11].

Droplet size distribution of SDS stabilized hexadecane emulsion in DI water and different aqua solutions were measured by light diffraction method. Smallest droplets were observed in 469mM NaCl concentration (measured smallest droplet range 0.479-0.550 $\mu\text{m}$ ). In model sea water, oil droplets' sizes were measured to be slightly bigger (measured smallest droplet range 0.631-0.724 $\mu\text{m}$ ) than 469mM NaCl concentration. Number- based droplet distribution demonstrated that ~70% of the droplets in model sea water and ~80% of the droplet in 469mM NaCl concentration were measured to be less than 1 $\mu\text{m}$ .

The emulsions with the concentrations of 6.7 mM and 54.3 mM  $\text{MgSO}_4$  represented similar droplet size. Smallest droplet size ranges 549.54 – 630.96 $\mu\text{m}$  and ~80% of the

droplets measured less than  $1\mu\text{m}$  in both emulsions. In DI water, smallest droplet range measured to be  $0.631\text{-}0.724\mu\text{m}$  and the number base distribution of droplets showed that  $\sim 70\%$  of droplets smaller than  $1\mu\text{m}$ .

The largest oil droplets were detected in  $54.3\text{ mM MgSO}_4$  concentrations (measured largest droplet range  $478.63\text{ - }549.54\mu\text{m}$ ) and DI water,  $6.7\text{ mM MgSO}_4$  and model sea water had second largest droplet with the range of  $363.08\text{ - }416.87\mu\text{m}$ . In  $469\text{ mM NaCl}$ , the largest droplet was measured in the range of  $91.20\text{ - }104.71\mu\text{m}$ .

Previous studies have reported the effect of salt on IFT [11, 22]. Presence of salt decreases liquid – liquid interfacial tension which promote the accumulation of the surfactant at the interface and hence resulted in IFT decrease [23]. Therefore, the addition of salt is expected to produce smaller oil droplets due to decrease in IFT. However, the relation between oil droplet and IFT was not parallel, because the addition of salt is also effective on droplet charge.

The  $\zeta$ - potential of hexadecane in the presence of  $0.1\text{ mM SDS}$  was measured to be  $-101\pm 22\text{ mV}$  in a previous study [11] and it was stated that addition of salt can significantly decrease the  $\zeta$  - potential. Therefore, because of two opposite effects, a linear correlation between droplet size and IFT could not be achieved.

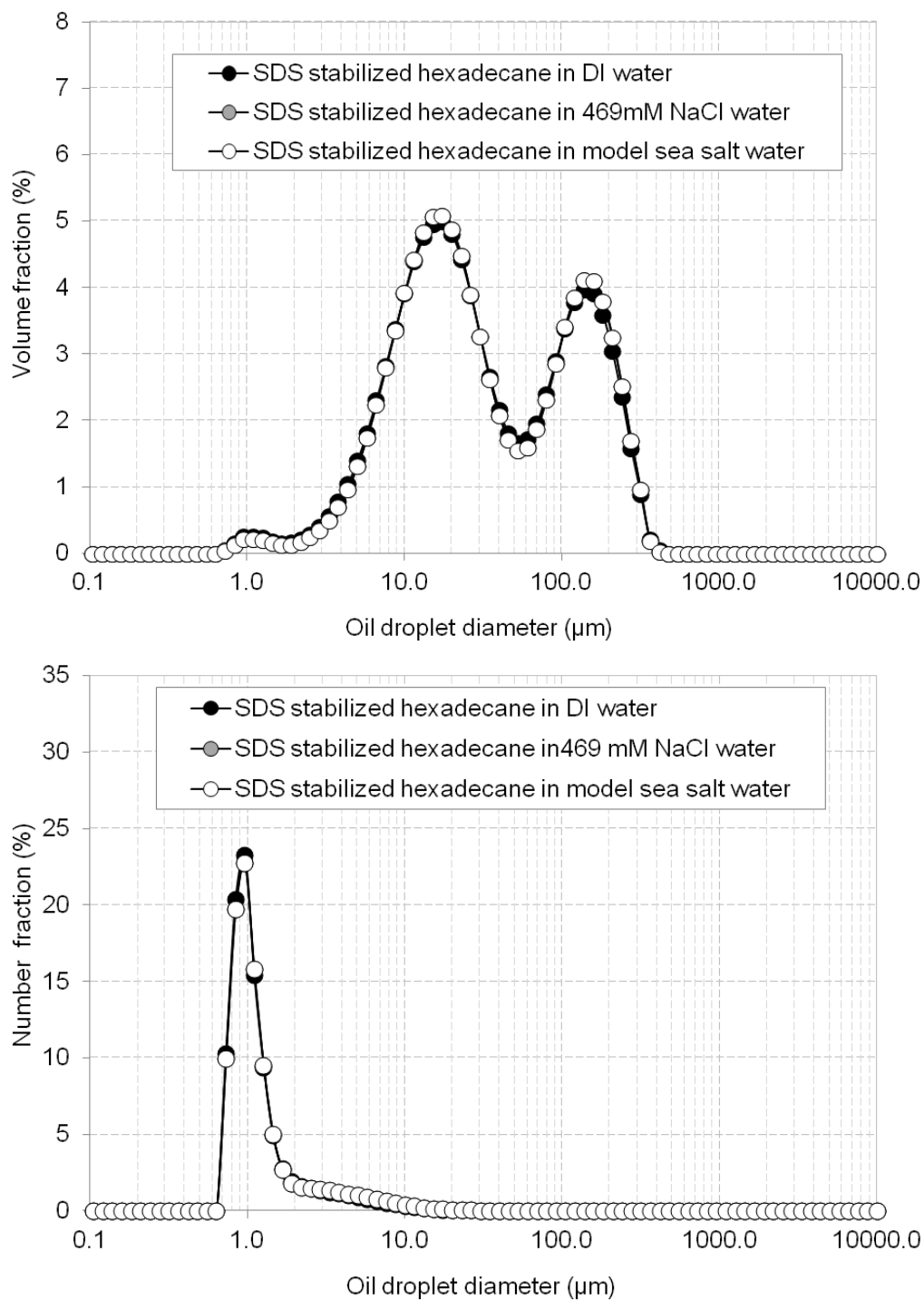


Figure 2.1: Volume and Number fraction (%) distributions for SDS-stabilized hexadecane-water emulsion 1000 μL(oil)/L, 0.1mM SDS in different salinities.

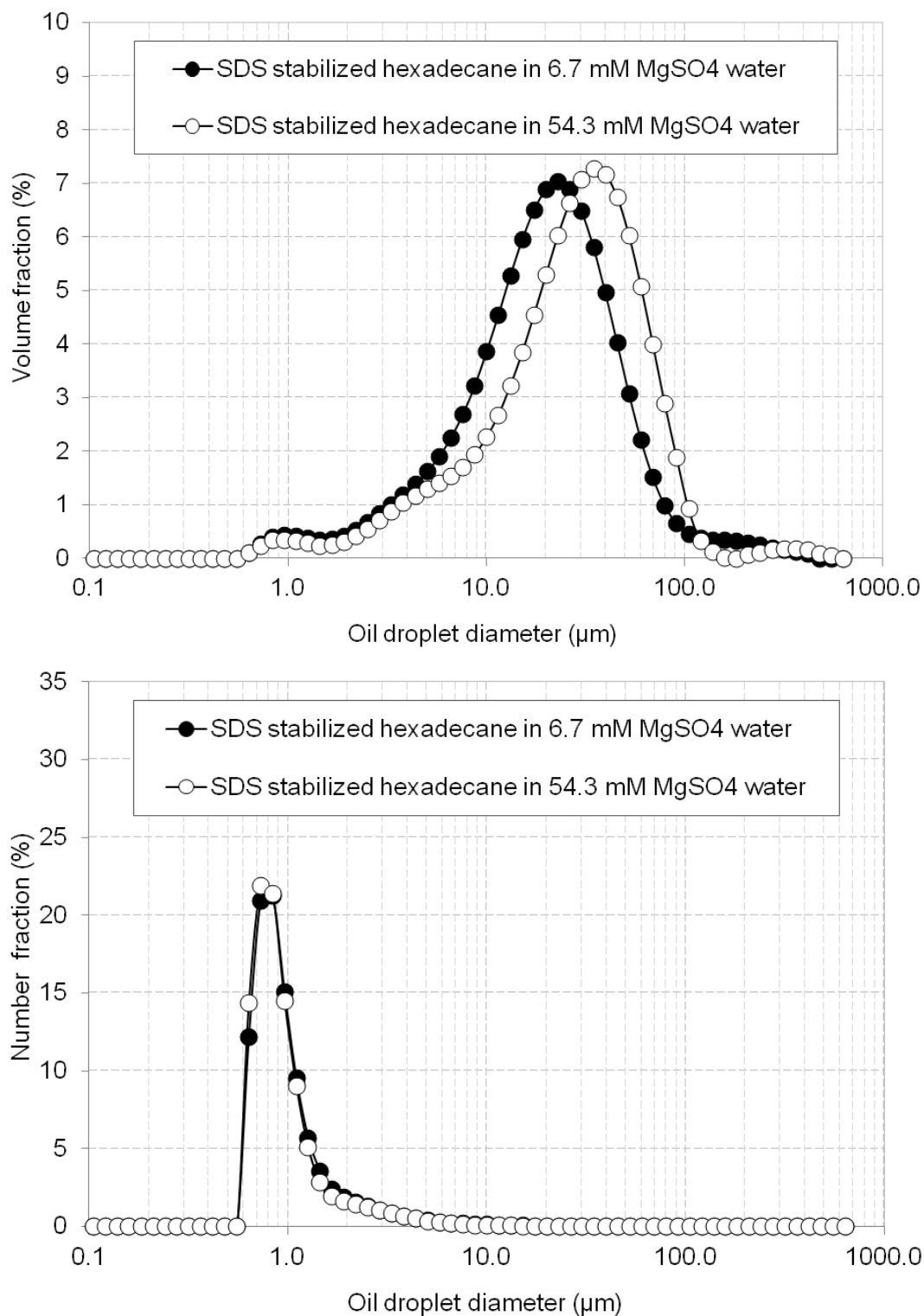


Figure 2.2: Volume and Number fraction (%) distributions for SDS-stabilized hexadecane-water emulsion 1000  $\mu\text{L}(\text{oil})/\text{L}$ , 0.1mM SDS in different salinity.

Contacts angle is one of the important parameters to understand attachment and displacement of the droplets at the interface. It determines the interaction energy between a liquid and a solid in a minimum distance between two surfaces [24] and it is the best way to characterize the wetting of a solid surface by a liquid [25]. The angle can be altered in the presence of salt and surfactant. For instance, salt can neutralize the negative charged solid surface and, at the same time it counteracts the hydrophilicity of the solid surface.

In our study, the contact angle ( $\theta$ ) of the hexadecane on the PTCA membrane in the 0.1mM SDS solution was measured to be  $122.76^\circ$  and it was used in the equation 1, in order to determine critical droplet size at 2Psi the pressure. This is the pressure used for dead-end microfiltration of the emulsions.

Since oil droplets can be deformed under pressure, rise in the transmembrane pressure can increase oil passage by forcing oil droplets through membrane pores. Therefore, it is important to determine critical pressure to prevent oil passage through the membrane. Additionally, operating the system in a transmembrane pressure below the critical pressure can minimize the membrane fouling [26].

In the equation 1 an oil droplet of diameter,  $d_{drop}$  and circular pore of diameter,  $d_{pore}$ , [26]:

$$\Delta P_{\text{crit}} = 4\sigma \frac{\cos \theta}{d_{\text{pore}}} \left[ 1 - \left( \frac{2 + 3 \cos \theta - \cos^3 \theta}{4 \left( \frac{d_{\text{drop}}}{d_{\text{pore}}} \right)^3 \cos^3 \theta - (2 - 3 \sin \theta + \sin^3 \theta)} \right)^{1/3} \right] \quad (1)$$

where  $\sigma$  is the interfacial tension and  $\theta = 180^\circ - \varphi$  where  $\varphi$  is the contact angle between the surface of the membrane and the oil droplet at the oil/water interface. Based on the equation,  $d_{\text{drop}}$  was calculated to be  $0.76\mu\text{m}$ . Thus, the droplet smaller than  $d_{\text{drop}}$  can pass through the membrane to the permeate side at 2 Psi even if they are larger than the membrane's pore size.

In the volume-base droplet size distribution of SDS stabilized emulsion in DI water, the volume ratio of the droplets smaller than  $0.76\mu\text{m}$  is about 0.13%. Thus, the predicted % oil rejection for DI water is 99.87%. However, oil rejection was measured to be %100 by gas chromatography. In other saline conditions, 100% oil rejections were observed, except 54.3 mM  $\text{MgSO}_4$  concentration. Its rejection was calculated to be 99.99%.

### 3.3.2 Assessing filterability of hexadecane

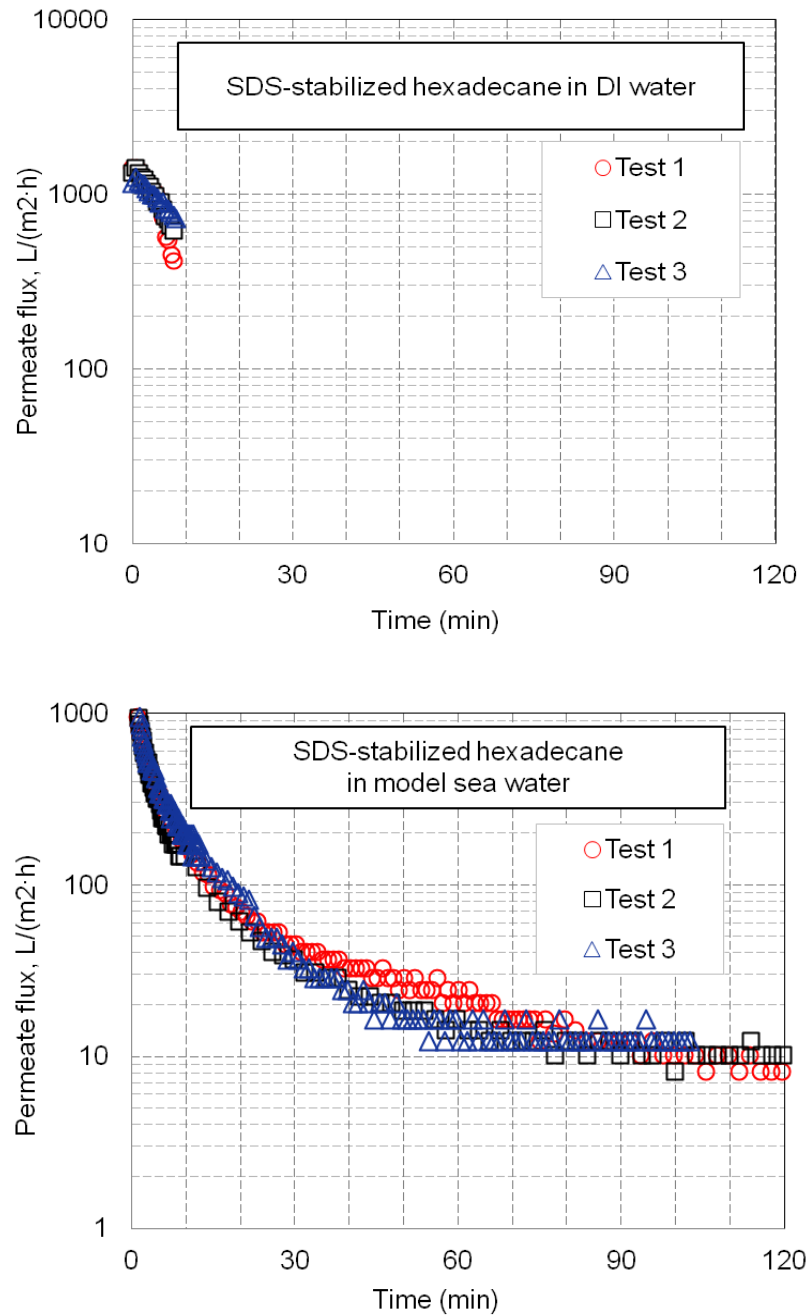


Figure 2.3: Permeate flux behavior in dead-end microfiltration tests with SDS-stabilized hexadecane emulsions in either DI or model sea water. The experiments were performed in a constant pressure regime ( $\Delta P = 2$  psi). The hydraulic resistance of membranes averaged over tests 1 – 3 with emulsions in DI and model water. Average hydraulic resistances of the membrane was  $(36 \pm 3) \cdot 10^9 \text{ m}^{-1}$



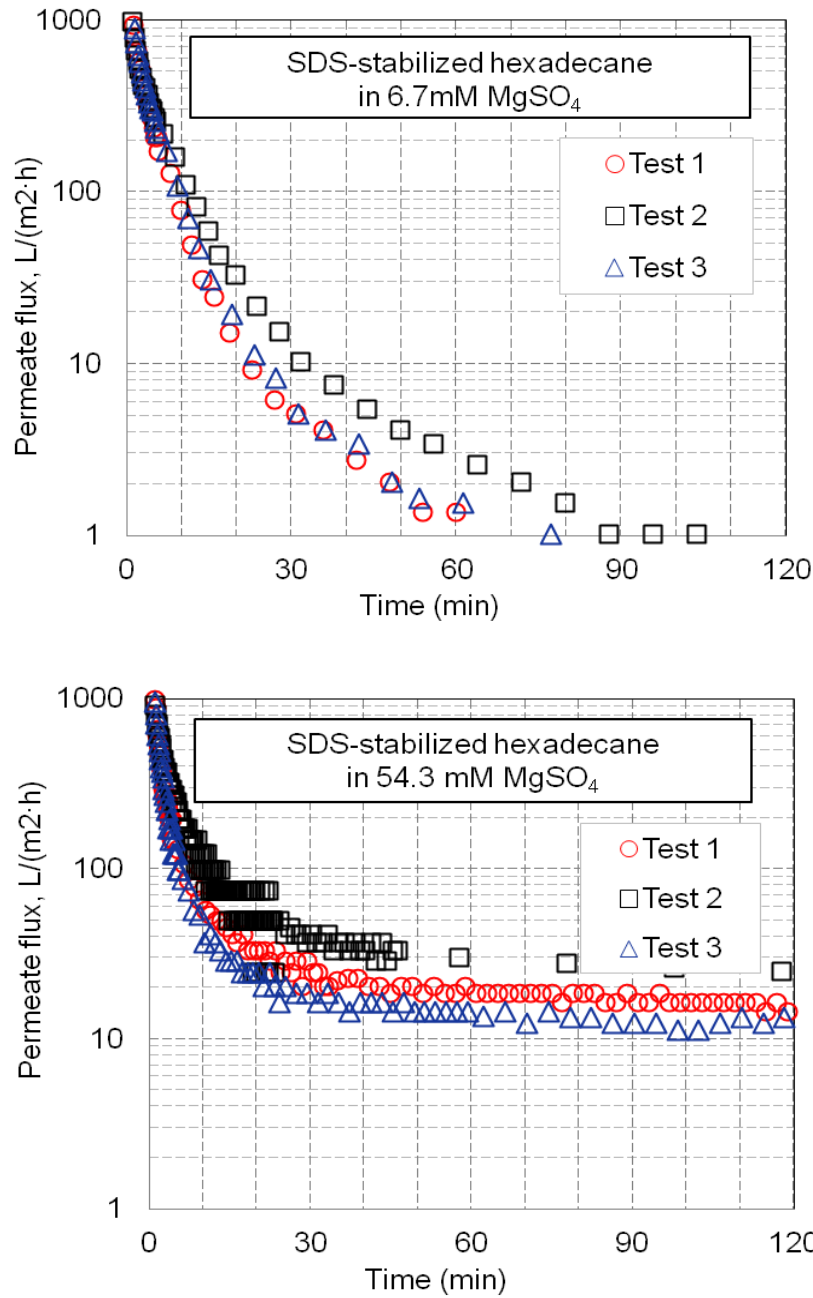


Figure 2.4: Permeate flux behavior in dead-end microfiltration tests with SDS-stabilized hexadecane emulsions in different  $\text{MgSO}_4$  concentrations. The experiments were performed in a constant pressure regime ( $\Delta P = 2$  psi). The hydraulic resistance of membranes averaged over tests 1 – 3 with emulsions in 6.7 mM  $\text{MgSO}_4$  and 54.3 mM  $\text{MgSO}_4$ . Average hydraulic resistances of the membrane was  $(33 \pm 2) \cdot 10^9 \text{ m}^{-1}$

Dead-end microfiltration experiments were performed at 2 psi constant pressure. Clean water flux test and then conditioning with DI water and aqua solutions in the presence of SDS were completed before each microfiltration experiment. During conditioning of the membrane, DI water and aqua solutions in the presence of SDS had constant fluxes. However, the fluxes of all solutions during conditionings observed higher than clean water fluxes at 2 psi due to increase in membrane hydrophilicity. Surfactant pretreatment alters the membrane surface more homogenously permeable decrease the surface rugosity, improve surface hydrophilicity. These changes on membrane surface mitigate locally the polarization around pores and reduce the hydrophobic sites on membrane for adhesion [27]. In Chapter 1, (pretreatment) conditioning performed with Corexit 9500 solutions and due to the changes on the membrane surface less fouling was observed.

The presence of salt in oil-water emulsion is known to alter the characteristics of the emulsion and membrane surface. Therefore, in this study, the emulsions with different salt concentrations were performed to investigate the effect of salt on the membrane fouling.

The filtration experiment of SDS stabilized emulsion in DI water represented the highest flux. All emulsion passed through the membrane about 7 min. The initial flux was observed  $1295 \pm 136 \text{ L}/(\text{m}^2 \cdot \text{h})$  and the last measured flux was  $633 \pm 91 \text{ L}/(\text{m}^2 \cdot \text{h})$ . However, in the case of 6.7 mM  $\text{MgSO}_4$  permeate flux sharply decreased. The initial flux  $1456 \pm 105 \text{ L}/(\text{m}^2 \cdot \text{h})$  and after 2 hours experiment, flux decreased to  $0.44 \pm 0.1 \text{ L}/(\text{m}^2 \cdot \text{h})$ . In

the presence of 54.3 mM  $\text{MgSO}_4$  and model sea salt, initial fluxes were measured to be  $1578 \pm 153 \text{ L}/(\text{m}^2 \cdot \text{h})$  and  $1508 \pm 8$ , respectively and end of the experiments, fluxes decreased to  $19 \pm 6 \text{ L}/(\text{m}^2 \cdot \text{h})$  and  $10 \pm 2 \text{ L}/(\text{m}^2 \cdot \text{h})$ , respectively. These imply that addition of salt practically increases the membrane fouling, but after some point, increase in salt concentration decreased the membrane fouling. Changes in membrane surface and oil droplet' characteristics might be the reason of different membrane fouling.

In DI water condition droplets are highly negatively charged and membrane surface also assumed to be about same charged with oil droplets. In this case, membrane-oil droplet surface interaction more repulsive than other conditions, so this could lead to high permeate flux.

In 6.7 mM  $\text{MgSO}_4$  concentration, the decline in permeate flux could be due to decrease in the charged. Less charged oil droplets could deposit on the membrane surface because of the less charged membrane surface which decreases the electrostatic repulsion between membrane surface and oil droplets.

Studies on salinity effect on anionic surfactant adsorption have reported that the presence of salt can increase the adsorption of surfactant on a negatively charged solid surface [28, 29]. Therefore, in the presence of high salt concentrations, which are 54.3 mM  $\text{MgSO}_4$  and model sea water, membrane surface could have more hydrophilic surface because of high salinity and this might be the reason higher fluxes compare to the emulsion in 6.7 mM  $\text{MgSO}_4$  concentration.

### 3.4. Conclusions

In this study, effects of salt concentration on membrane fouling were investigated. Hexadecane in water emulsions in various salt concentrations were characterized regarding droplet size distribution and interfacial tension. A clear trend cannot be observed between droplet size distribution and droplet size of hexadecane. In all emulsions, more than %70 of the droplets was measured to be less than 1  $\mu\text{m}$ .

Interfacial tension between hexadecane and water decreased with the addition of salt.

During microfiltration of the emulsions, while the lowest flux observed in 6.7 mM  $\text{MgSO}_4$  concentration, the highest flux was observed in DI water condition. In practical addition of salt decreased the flux, but the amount of the salt has determinant effect on membrane fouling. Because of the decrease in electrostatic attraction between membrane and oil droplets, more fouling was observed in the emulsion with the concentration of 6.7 mM  $\text{MgSO}_4$ .

## APPENDIX D

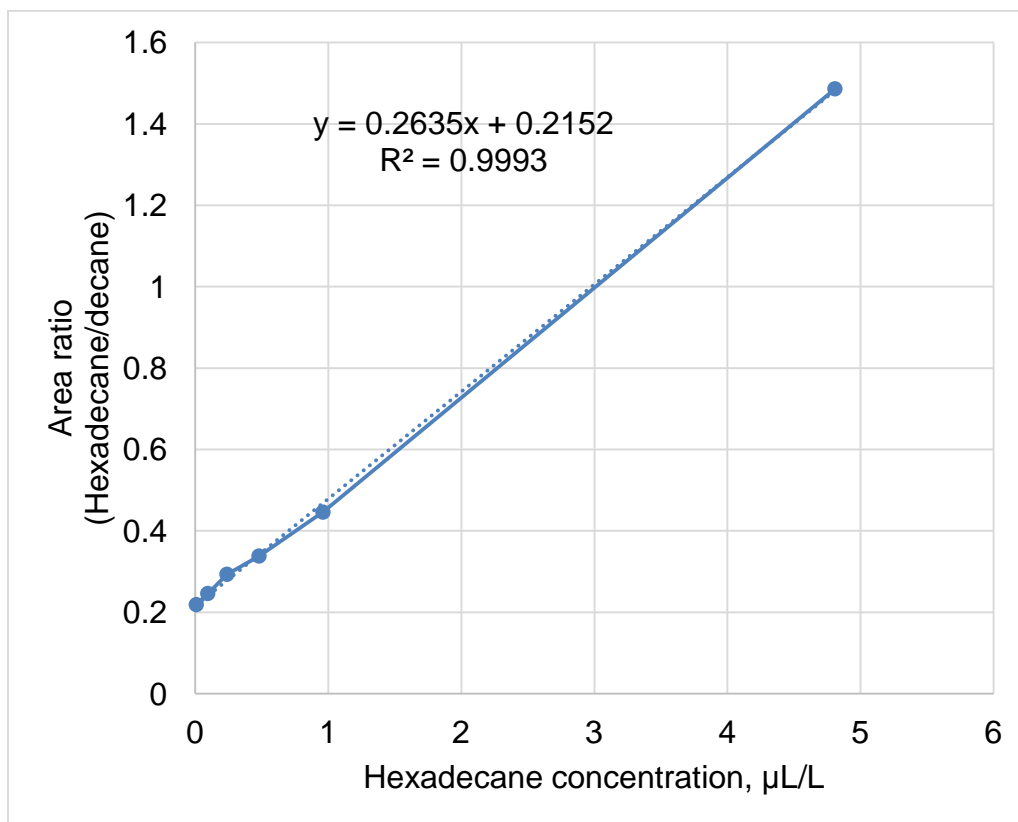


Figure D.1: Calibration curve for hexadecane concentration determination

## REFERENCES

## REFERENCES

- [1] L.Y. Susan, S. Ismail, B.S. Ooi, H. Mustapa, Surface morphology of pvdf membrane and its fouling phenomenon by crude oil emulsion, *Sustainable WaterEngineering*, 15 (2017) 55-61.
- [2] J.W. Patterson, *Industrial Wastewater Treatment Technology*, Second edition ed., 1985.
- [3] D.M. Patten, Intra-industry environmental disclosures in response to the Alaskan oil spill: A note on legitimacy theory, 17 (1992) 471-475.
- [4] R. Weisberg, L. Zheng, Y. Liu, *On the Movement of Deepwater Horizon Oil to Northern Gulf Beaches*, 2017.
- [5] E. Kujawinski, B.K. Elizabeth, C.K.S. Melissa, L.V. David, K.B. Angela, Fate of Dispersants Associated with the Deepwater Horizon Oil Spill, *Environmental science & technology*, 45.
- [6] K.C. Powell, A. Chauhan, Dynamic interfacial tension and dilational rheology of dispersant Corexit 9500, *Colloids and surfaces. A, Physicochemical and engineering aspects*, 497 352-361.
- [7] M. Cheryan, N. Rajagopalan, Membrane processing of oily streams. *Wastewater treatment and waste reduction*, 151 (1998) 13-28.
- [8] M. Hesampour, A. Krzyzaniak, M. Nyström, The influence of different factors on the stability and ultrafiltration of emulsified oil in water, 325 (2008) 199-208.
- [9] N.G.P. Chew, S. Zhao, C.H. Loh, N. Permogorov, R. Wang, Surfactant effects on water recovery from produced water via direct-contact membrane distillation, 528 (2017) 126-134.
- [10] H.J. Tanudjaja, V.V. Tarabara, A.G. Fane, J.W. Chew, Effect of cross-flow velocity, oil concentration and salinity on the critical flux of an oil-in-water emulsion in microfiltration, 530 (2017) 11-19.
- [11] E.N. Tummons, J.W. Chew, A.G. Fane, V.V. Tarabara, Ultrafiltration of saline oil-in-water emulsions stabilized by an anionic surfactant: Effect of surfactant concentration and divalent counterions, 537 (2017) 384-395.
- [12] Z. He, S. Kasemset, A.Y. Kirschner, Y.-H. Cheng, D.R. Paul, B.D. Freeman, The effects of salt concentration and foulant surface charge on hydrocarbon fouling of a poly(vinylidene fluoride) microfiltration membrane, 117 (2017) 230-241.

- [13] X. Zhu, A. Dudchenko, X. Gu, D. Jassby, Surfactant-stabilized oil separation from water using ultrafiltration and nanofiltration, *Journal of membrane science*, 529 159-169.
- [14] R.L. Pitre, Produced Water Discharges into Marine Ecosystems, Offshore Technology Conference, (1984).
- [15] S. Paria, K.C. Khilar, A review on experimental studies of surfactant adsorption at the hydrophilic solid–water interface, 110 (2004) 75-95.
- [16] M.J. Rosen, K.J. T., *Surfactants and Interfacial Phenomena*, 2012.
- [17] F.O. Opawale, D.J. Burgess, Influence of Interfacial Properties of Lipophilic Surfactants on Water-in-Oil Emulsion Stability, 197 (1998) 142-150.
- [18] G. Chen, D. Tao, An experimental study of stability of oil–water emulsion, 86 (2005) 499-508.
- [19] M. Nyström, Ultrafiltration of O/W emulsions stabilized by limiting amounts of tall oil, 57 (1991) 99-114.
- [20] J.A. Brant, A.E. Childress, Assessing short-range membrane–colloid interactions using surface energetics, 203 (2002) 257-273.
- [21] E.N. Tummons, V.V. Tarabara, Jia W. Chew, A.G. Fane, Behavior of oil droplets at the membrane surface during crossflow microfiltration of oil–water emulsions, 500 (2016) 211-224.
- [22] S. Kumar, A. Mandal, Studies on interfacial behavior and wettability change phenomena by ionic and nonionic surfactants in presence of alkalis and salt for enhanced oil recovery, 372 (2016) 42-51.
- [23] A. Bera, K. S, K. Ojha, T. Kumar, A. Mandal, Mechanistic Study of Wettability Alteration of Quartz Surface Induced by Nonionic Surfactants and Interaction between Crude Oil and Quartz in the Presence of Sodium Chloride Salt, *Energy & Fuels*, 26 (2012) 3634-3643.
- [24] C.J.v. Oss, *Interfacial Forces in Aqueous Media*, Second edition ed., 2006.
- [25] R. Pichot, F. Spyropoulos, I.T. Norton, Competitive adsorption of surfactants and hydrophilic silica particles at the oil–water interface: Interfacial tension and contact angle studies, 377 (2012) 396-405.
- [26] F.F. Nazzari, M.R. Wiesner, Microfiltration of oil-in-water emulsions, *Water Environ. Res.*, 68 (1996) 1187-1191.



- [27] A.G. Fane, C.J.D. Fell, K.J. Kim, The effect of surfactant pretreatment on the ultrafiltration of proteins, *Proceedings of the Symposium on Membrane Technology*, 53 (1985) 37-55.
- [28] S. Paria, C. Manohar, K.C. Khilar, Kinetics of Adsorption of Anionic, Cationic, and Nonionic Surfactants, *Industrial & Engineering Chemistry Research*, 44 (2005) 3091-3098.
- [29] S. Paria, C. Manohar, K. C Khilar, *Experimental Studies on Adsorption of Surfactants Onto Cellulosic Surface and its relevance to Detergency*, 2003.